

Est.
1841

YORK
ST JOHN
UNIVERSITY

Glendell, M., Jones, R., Dungait, J.A.J., Meusburger, K., Schwendel, Arved ORCID logo ORCID: <https://orcid.org/0000-0003-2937-1748>, Barclay, R., Barker, S., Haley, S., Quine, T. A. and Meersmans, J. (2018) Tracing of particulate organic C sources across the terrestrial-aquatic continuum, a case study at the catchment scale (Carminowe Creek, southwest England). *Science of the total environment*, 616-7. pp. 1077-1088.

Downloaded from: <https://ray.yorks.ac.uk/id/eprint/2602/>

The version presented here may differ from the published version or version of record. If you intend to cite from the work you are advised to consult the publisher's version:

<https://www.sciencedirect.com/science/article/pii/S0048969717329303>

Research at York St John (RaY) is an institutional repository. It supports the principles of open access by making the research outputs of the University available in digital form. Copyright of the items stored in RaY reside with the authors and/or other copyright owners. Users may access full text items free of charge, and may download a copy for private study or non-commercial research. For further reuse terms, see licence terms governing individual outputs. [Institutional Repository Policy Statement](#)

RaY

Research at the University of York St John

For more information please contact RaY at ray@yorks.ac.uk

1 **Tracing of particulate organic C sources across the terrestrial-aquatic continuum, a**
2 **case study at the catchment scale (Carminowe Creek, South West England)**

3 M. Glendell^{1*}, R. Jones², J.A.J. Dungait³, K. Meusburger⁴, A.C. Schwendel⁵, R. Barclay², S.
4 Barker⁶, S. Haley², T.A. Quine², J. Meersmans⁷

5 (1) The James Hutton Institute, Craigiebuckler, Aberdeen AB15 8QH, UK

6 (2) University of Exeter, Geography - College of Life and Environmental Sciences, Exeter
7 EX4 4RJ, UK

8 (3) Sustainable Agriculture Science, Rothamsted Research, North Wyke, Okehampton,
9 Devon, EX20 2SB, UK

10 (4) Environmental Geosciences, University of Basel, Bernoullistrasse 30, 4056 Basel,
11 Switzerland

12 (5) School of Humanities, Religion & Philosophy, York St John University, Lord Mayor's
13 Walk, York, YO31 7EX, UK

14 (6) Environment and Sustainability Institute, University of Exeter, Penryn Campus, Penryn,
15 Cornwall TR10 9FE

16 (7) School of Water, Energy and Environment, Cranfield University, Bedford, MK43 0AL,
17 UK

18 * Corresponding author: The James Hutton Institute, Craigiebuckler, Aberdeen AB15 8QH,
19 Scotland, UK, Miriam.Glendell@hutton.ac.uk, tel: +44(0)1224 395 320, fax: +44 (0)844 928
20 5429

21 **Abstract**

22 Soils deliver crucial ecosystem services, such as climate regulation through carbon (C)
23 storage and food security, both of which are threatened by climate and land use change.
24 While soils are important stores of terrestrial C, anthropogenic impact on the lateral fluxes of
25 C from land to water remains poorly quantified and not well represented in Earth system
26 models. In this study, we tested a novel framework for tracing and quantifying lateral C
27 fluxes from the terrestrial to the aquatic environment at a catchment scale. The combined use
28 of conservative plant-derived geochemical biomarkers *n*-alkanes and bulk stable $\delta^{13}\text{C}$
29 and $\delta^{15}\text{N}$ isotopes of soils and sediments within an inter-disciplinary framework allowed us to
30 distinguish between particulate organic C sources from different land uses (i.e. arable and
31 temporary grassland *vs.* permanent grassland *vs.* riparian woodland *vs.* river bed sediments)
32 ($p < 0.001$), showing an enhanced ability to distinguish between land use sources as compared
33 to using just biomarkers alone. The terrestrial-aquatic proxy (TAR) ratio derived from *n*-
34 alkane signatures indicated an increased input of terrestrial-derived organic matter (OM) to
35 lake sediments over the past 60 years, with an increasing contribution of woody vegetation
36 over time. This may be related to agricultural intensification, leading to enhanced soil

37 erosion, but also an increase in riparian woodland that may disconnect OM inputs from arable
38 land uses in the upper parts of the study catchment. Spatial variability of geochemical proxies
39 showed a close coupling between OM provenance and riparian land use, supporting the new
40 conceptualization of river corridors (active river channel and riparian zone) as critical zones
41 linking the terrestrial and aquatic C fluxes. Further testing of this novel tracing technique
42 shows promise in terms of quantification of lateral C fluxes as well as targeting of effective
43 land management measures to reduce soil erosion and promote OM conservation in river
44 catchments.

45 **Keywords:** lateral carbon fluxes, sediment fingerprinting, biomarkers, *n*-alkanes, bulk stable
46 ¹³C and ¹⁵N isotopes

47

48 1. Introduction

49 Soils are critical to human wellbeing and deliver crucial ecosystem services, including
50 climate regulation and food security (Adhikari and Hartemink, 2016; Mouchet et al., 2016).
51 However, since the onset of agriculture, human activities have greatly altered soil processes
52 at a global scale, with consequences for the essential functions of soils to sequester and store
53 carbon (C), recycle nutrients and resist soil erosion (Amundson et al., 2015). As soils
54 represent the largest terrestrial store of organic C, more than three times as much as either the
55 atmosphere or terrestrial vegetation (Schmidt et al., 2011), these anthropogenic interventions
56 have also impacted the scale of the lateral fluxes of C from land to inland waters (Lauerwald
57 et al., 2015; Tian, 2015; Wohl et al., 2017).

58 However, the fluxes of C from land to ocean remain poorly quantified and not fully
59 accounted for in the current generation of Earth system models (Regnier et al., 2013). While
60 over the past decade, the understanding of rivers has been revised from ‘inert pipes’ simply
61 transporting C from land to the ocean to ‘active agents’, which play a crucial role in receiving,
62 transporting and processing C equivalent to net terrestrial primary production in their
63 watersheds (Aufdenkampe et al., 2011; Battin et al., 2009; Cole et al., 2007; Wohl et al.,
64 2017)., the magnitude, spatiotemporal patterns and controls on C fluxes from land to ocean
65 remain poorly quantified (Regnier et al., 2013; Wohl et al., 2017). While there is a growing
66 understanding of the magnitude of global C exports from rivers to the ocean (Li et al., 2017;
67 Ludwig et al., 2011; Tian et al., 2015), estimates of CO₂ evasion from inland waters
68 (Lauerwald et al., 2015; Raymond et al., 2013) and sediment burial in aquatic ecosystems
69 (Maavara et al., 2017; Tranvik et al., 2009) are still uncertain. However, the largest
70 uncertainties are associated with the scale of the total lateral C fluxes from land to inland
71 waters, with recent research suggesting that previous estimates may have largely over-
72 estimated C accumulation in terrestrial ecosystems (the terrestrial C sink) due to under-
73 estimation of this lateral C export (Nakayama, 2017). Therefore, there is a need to better
74 understand the scale of the anthropogenic impact on these lateral C fluxes from land to water
75 (Regnier et al., 2013; Wohl et al., 2017), as well as the processes involved in the loss and
76 preservation of C along the terrestrial-aquatic continuum (Marín-Spiotta et al., 2014), to

77 properly represent these processes and predict the present and future contribution of aquatic
78 C fluxes to the global C budget (Aufdenkampe et al., 2011; Battin et al., 2009; Cole et al.,
79 2007; Regnier et al., 2013).

80 Over the past decades, the awareness of the importance of soils in the functioning of many
81 vital ecosystem services, including climate change mitigation, food security, water resource
82 management and flood protection has greatly increased (Schroter et al., 2005). Nevertheless,
83 in many parts of the world where soil erosion rates exceed soil production, the sustainable
84 provision of these ecosystem services is under pressure (Alewell, et al., 2015; Amundson et
85 al., 2015; Panagos et al., 2015; Verheijen et al., 2009). The intensification of agriculture,
86 particularly over the past 60 years, has led to an exponential increase in sediment and organic
87 matter (OM) fluxes within agricultural catchments (Glendell and Brazier, 2014; Graeber et
88 al., 2015), with important consequences for on-site impacts, such as soil productivity, and
89 off-site impacts, in terms of nutrient pollution and sedimentation of water bodies (Tilman et
90 al., 2002). Hence, conservation of soil organic matter (SOM; which contains ~60% SOC)
91 remains critical for sustaining soil productivity and food security in a changing world
92 (Amundson et al., 2015) and for mitigating the acknowledged wide-scale impacts of
93 enhanced sedimentation and associated nutrient pollution on the ecological status of water
94 bodies and drinking water quantity and quality (Bilotta and Brazier, 2008; Glendell et al.,
95 2014a; Rickson, 2014; Schoumans et al., 2014).

96 Tracing and quantifying the sources of sediment and particulate organic C in the fluvial
97 environment is, therefore, key to supporting sustainable land management decisions and
98 maintaining ecosystem services. To date, most tracing techniques to apportion sediment
99 sources in fluvial environments applied in river management studies have used physical
100 sediment characteristics, geochemical properties, fallout radionuclides or mineral magnetic
101 properties. However, these tracers are not able to distinguish sources between specific land
102 uses, which are essential to inform mitigation measures and catchment management (Guzman
103 et al., 2013; Owens et al., 2016; Smith et al., 2015; Walling, 2013). Conversely, examination
104 of the provenance of sediment-bound OM using plant-specific biomarkers has been
105 established in paleo-ecological and marine sciences for some time (e.g. Galy et al., 2011;
106 Meyers and Lallier-Vergès, 1999; Meyers, 2003; Tolosa et al., 2013; Zech et al., 2012).
107 While a number of studies to date have sought to apply one or more biomarkers to understand
108 lateral C dynamics at the continental margins (e.g. Feng et al., 2015; Galy et al., 2011; Tao et
109 al., 2016), few studies have applied this approach to inland waters, especially headwaters,
110 which may cumulatively play an important role in lateral C export due to their spatial extent
111 and close terrestrial – aquatic coupling. Therefore the application of biomarkers, especially
112 aliphatic (saturated straight-chained) compounds such as *n*-alkanes (Chen et al., 2016, 2017;
113 Cooper et al., 2015; Puttock et al., 2014) and *n*-carboxylic acids (fatty acids) (Alewell et al.,
114 2016; Blake et al., 2012; Reiffarth et al., 2016), is now being examined as a new potential
115 tool for attribution of sediment and C provenance in river catchments, with a potential to
116 attribute organic matter sources to specific land uses, such as forest, arable and pasture.

117 *N*-alkanes are naturally occurring hydrocarbons which are relatively recalcitrant and more
118 resistant to microbial decomposition than other functionalized plant-derived lipids, e.g. fatty

119 acids or sterols (Ranjan et al., 2015). They are vegetation-specific neutral lipids derived from
120 plant waxes with different numbers of C atoms in the aliphatic molecule that are indicative of
121 different provenances of OM (Eglinton, 1962). In general, long-chain (C₂₇-C₃₁) *n*-alkanes are
122 derived from epicuticular plant waxes of terrestrial plants (Galy et al., 2011; Puttock et al.,
123 2014), medium chain-length (C₂₁-C₂₅) *n*-alkanes are produced by lower plants and aquatic
124 macrophytes (Fang et al., 2014; Meyers, 2003; Tolosa et al., 2013), while short chain-length
125 (C₁₅-C₁₉) *n*-alkanes are typically derived from aquatic algae (Meyers, 2003). Both individual
126 *n*-alkanes as well as different chain-length ratios have been used in paleo-ecological studies
127 to attribute OM sources over decadal to millennial timescales (Ranjan et al., 2015; Zech et
128 al., 2013, 2012). As *n*-alkane signatures are altered by land use change, they are ideally suited
129 to track changing OM sources from eroded soils and sediments over time (Chen et al., 2016).

130 With these naturally occurring biomarkers (and their compound-specific isotopic signatures
131 where vegetation sources with contrasting $\delta^{13}\text{C}$ values are evident) emerging as the new
132 potential tools for tracing of SOM in catchment studies, a key challenge lies in establishing
133 their effectiveness to act as land-management specific tracers of fluvial OM over decadal
134 timescales (Alewell et al., 2016; Cooper et al., 2015). As these new techniques are still in
135 their infancy (Owens et al., 2016) and require further development and testing, in this work
136 we aim to investigate the suitability of *n*-alkane biomarkers within an inter-disciplinary
137 context, beyond the traditional confines of soil science alone (Brevik et al., 2015; Owens et
138 al., 2016; Smith et al., 2015).

139 Therefore, this pilot study aims to evaluate the combined use of *n*-alkanes, bulk stable $\delta^{13}\text{C}$
140 and $\delta^{15}\text{N}$ isotopes and their ratios (Collins, et al., 2014, 2013; Meyers and Lallier-Vergès,
141 1999; Meyers, 2003; Ranjan et al., 2015) to advance the current understanding of the
142 temporal variability of lateral C fluxes from the terrestrial to the aquatic ecosystem in
143 relation to changing land management practices, over the past century. Our aims were to i)
144 test the ability of conservative *n*-alkane biomarkers and soil and sediment bulk stable $\delta^{13}\text{C}$
145 and $\delta^{15}\text{N}$ isotopes to distinguish between terrestrial and aquatic OM sources, ii) understand
146 the impact of land use on the spatial variability of OM provenance in river bed sediments and
147 iii) on OM accumulation in lake bed sediments, iv) test a methodology for quantifying the
148 temporal variability and the magnitude of lateral C fluxes from land to water at catchment
149 scales.

150

151 **2. Material and Methods**

152 2.1 Study site

153 The Carminowe Creek study catchment, located in southwest England (50°4' W 5°16'),
154 covers c. 4.8 km² at an altitude range of 0-80 m above sea level (Fig. 1). The catchment outlet
155 drains into a large freshwater lake Loe Pool (50 ha) that is separated from the Atlantic Ocean
156 by a natural shingle barrier, thus creating a relatively closed natural hydrological system. The
157 study catchment comprises two main streams (Northern and Southern subcatchments) with a
158 joint outlet into the south-western branch of Loe Pool. The average total annual rainfall is

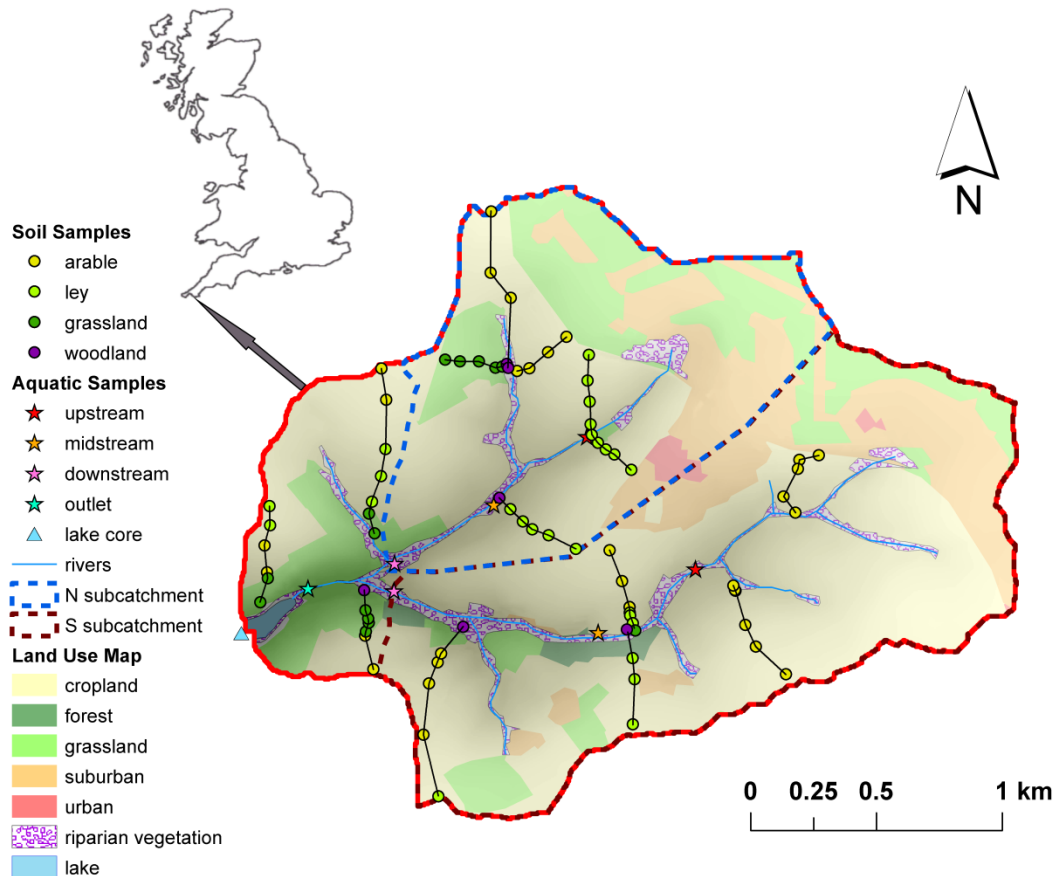
159 approximately 1000 mm and mean annual temperature is approximately 11°C
160 (<http://www.metoffice.gov.uk/public/weather/climate/>). Bedrock geology comprises silt-,
161 sand- and mudstone (<http://mapapps.bgs.ac.uk/geologyofbritain/home.html>), which is
162 overlaid by freely draining loamy soils (Soil Survey of England and Wales, 1983). Land use
163 on the catchment plateaux is dominated by cropland in rotation of arable crops and temporary
164 grassland (also referred to as grass ley), while permanent grassland is found on steeper
165 hillslopes, with riparian vegetation (mostly wet woodland dominated by willow *Salix sp.*,
166 alder *Alnus glutinosa* and wet grassland) located in the riparian zone within the river corridor.

167

168 2.2 Field sampling

169

170 78 soil cores were taken 14 hillslope transects across the two sub-catchments (8 cm diameter,
171 depth 0-15 cm), covering the topographic sequence from plateaux, convex, steep slope,
172 concave and footslope locations. In total, 31 samples were taken from arable land use, 26
173 from temporary grassland (ley), 14 from permanent grassland and 7 from riparian woodland.
174 Three river-bed sediment samples were collected with a hand trowel and bulked into a single
175 sample on a single occasion at 7 locations along each of the two streams at an (i) upstream
176 (ii) midstream and (iii) downstream location and the joint catchment outlet before the
177 confluence with Loe Pool. Two 0.5 m deep lake sediment cores were taken from Loe Pool c.
178 150 m below the outlet of Carminowe Creek using a Mackereth corer (Mackereth, 1969).



179

180 Fig. 1 The study site location in south-west England showing land use, the 14 study transects,
 181 river bed sediment sampling locations and the lake core.

182

183 2.3 Laboratory analysis

184 Following sample collection, river bed and lake core sediment samples were stored at 4°C
 185 and analysed as soon as possible. Soil samples were oven dried at 40°C and sieved to <2 mm
 186 and >2 mm fractions. River bed samples were wet sieved at 250 µm to separate coarse
 187 vegetation debris as in Galy et al. (2011) and the < 250 µm fraction was oven dried at 40°C
 188 and retained for further analysis. The lake sediment core was sliced into 2 cm increments and
 189 freeze dried.

190 All soil, river bed sediment and lake core samples were analysed for total C, N and bulk $\delta^{13}\text{C}$
 191 and $\delta^{15}\text{N}$ using a SerCon Integra2 isotope ratio mass spectrometer (SerCon Ltd., Crewe, UK).
 192 An in house standard of Alanine (N=16.7%, C=40%, $\delta^{15}\text{N}=-1.68\text{‰}_{\text{AIR}}$, and $\delta^{13}\text{C}=-$
 193 $19.58\text{‰}_{\text{VPDB}}$) was used in duplicate every 9 samples to provide quality control and to act as
 194 an internal reference. This was calibrated within each analytical run by also analysing
 195 International Atomic Energy Agency (IAEA) reference materials N-1 and N-2 for nitrogen
 196 and CH-6 and LSVEC for carbon. Due to systematic blanks data had to be blank subtracted
 197 and a linearity correction was applied based on the analysis of the IAEA reference materials.
 198 The analytical precision of the internal quality control samples of alanine was determined.

199 The standard deviation of the $\delta^{15}\text{N}$ measurements was $<0.3\text{‰}$ and of the $\delta^{13}\text{C}$ measurements
200 was $<0.1\text{‰}$. The values were expressed relative to AIR and Vienna PeeDee Belemnite
201 (VPDB) for nitrogen and carbon respectively. The formula used for presenting δ values is as
202 follows:

$$203 \quad \delta^{15}\text{N} \text{ X } \text{‰}_{\text{AIR}} = (\text{R}_{\text{sam}}/\text{R}_{\text{ref}})-1)*1000 \quad (1)$$

$$204 \quad \delta^{13}\text{C} \text{ X } \text{‰}_{\text{VPDB}} = (\text{R}_{\text{sam}}/\text{R}_{\text{ref}})-1)*1000 \quad (2)$$

205 Where sam is sample and ref is the reference material, R is the ratio of the heavy isotope over
206 the light isotope, X being the isotope ratio expressed in units of per mille (‰).

207 In order to establish a chronology for the lake core profile, ^{137}Cs assay of individual 2 cm
208 core sections was undertaken at 661.67 KeV using an ORTEC GMX co-axial HPGe γ -
209 detector, coupled to a multi-channel analyser. Sample count times were generally 24 hours,
210 resulting in analytical precision of c. 5%.

211 On the basis of likely hydrological connectivity with the watercourses we selected a sub-set
212 of 50 samples to estimate *n*-alkane concentrations ($\mu\text{g g}^{-1}\text{ C}$) from soil samples Lake core
213 samples were combined into 4 cm increments. . The procedure of total lipid extraction was
214 followed by lipid fractionation to isolate the hydrocarbon fraction for analysis using an
215 Agilent 6890 GC instrument coupled to an Agilent 5973 MS instrument and equipped with an
216 Agilent DB-5 ms column (30 m x 250 μm i.d.x 0.25 μm film thickness). The dominant
217 fragment ions (base peak) were represented by *m/z* 57 and the diagnostic ions (*m/z*) 282
218 (C_{20}), 296 (C_{21}), 324 (C_{23}), 338 (C_{24}), 352 (C_{25}), 366 (C_{26}), 380 (C_{27}), 394 (C_{28}), 408 (C_{29}),
219 422 (C_{30}), 436 (C_{31}), 450 (C_{32}), 464 (C_{33}) and 478 (C_{34} , internal standard) (Norris, 2013). The
220 concentrations of individual *n*-alkanes were determined relative to the C_{34} internal standard.

221 Interpretation of *n*-alkane results used the percentage of C_{27} , C_{29} and C_{31} calculated as (Torres
222 et al., 2014):

$$223 \quad \% \text{ C}_i = \text{C}_i / (\text{C}_{27} + \text{C}_{29} + \text{C}_{31}) \quad (3)$$

224 where C_i stands for the respective *n*-alkane (C_{27} , C_{29} and C_{31}).

225 Further, we used the ratio between the shorter chain C_{27} (indicative of woody source (Zech et
226 al., 2009) and longer chain C_{31} (indicative of grass source (Eckmeier and Wiesenberg, 2009)
227 to distinguish between respective contributions of OM from woodland and grassland land
228 uses (Puttock et al., 2014).

229

230 2.4 Indicators of aquatic versus terrestrial OM sources

231 To interpret the relative contribution of higher aquatic vs. terrestrial plants to OM in river and
232 lake sediments we used the following formula (Ficken et al., 2000):

$$233 \quad \text{PAQ} = \frac{(\text{C}_{23} + \text{C}_{25})}{(\text{C}_{23} + \text{C}_{25} + \text{C}_{29} + \text{C}_{31})} \quad (4)$$

234 where PAQ is the ratio of shorter-chain *n*-alkanes (C₂₃+C₂₅) contributed by higher aquatic
235 plants (macrophytes) and mosses to the concentration (in µg g⁻¹) of *n*-alkanes indicative of
236 both aquatic and terrestrial vegetation (C₂₃+C₂₅+C₂₉+C₃₁).

237 The proportion of OM from terrestrial sources in river bed sediments and in the lake core was
238 calculated using the following formula (Fang et al., 2014; Meyers, 2003)

$$239 \text{ TAR} = \frac{(C_{27}+C_{29}+C_{31})}{(C_{15}+C_{17}+C_{19})} \quad (5)$$

240 where TAR is terrestrial/aquatic ratio of the concentration of *n*-alkanes (in µg g⁻¹) derived
241 from terrestrial sources (C₂₇+C₂₉+C₃₁) to those indicative of aquatic algae (C₁₅+C₁₇+C₁₉).

242 Organic matter degradation in the lake core was examined using the odd-over-even
243 predominance (OEP) *n*-alkane ratio (Zech et al., 2013) as follows:

$$244 \text{ OEP} = (nC_{27} + nC_{29} + nC_{31} + nC_{33}) / (nC_{28} + nC_{30} + nC_{32}) \quad (6)$$

245 High OEPs point either to an increased OM input and/or to an increased OM preservation
246 while low OEPs are indicative of accelerated degradation under aerobic conditions (Zech et
247 al., 2013).

248 We used δ¹³C, δ¹⁵N and C/N ratio as further geochemical proxies to understand the
249 proportion of OM contributed by algal vs. terrestrial plant derived production as used in
250 previous studies (Fang et al., 2014; Hamilton and Lewis, 1992; Meyers, 2003).

251

252 2.5 Statistical Analysis

253 Kruskal-Wallis non-parametric test was used to examine the differences between elemental
254 (C/N) and isotopic (δ¹⁵N, δ¹³C) signatures between different sediment sources. All soil, river
255 bed sediment and lake core increments were included in this analysis. Principal component
256 analysis (PCA) was used to examine whether elemental and *n*-alkane ratios could be used to
257 distinguish the provenance of sediment sources derived from six potential sources (arable,
258 temporary grassland (ley), permanent grassland, riparian woodland, lake or river bed). All
259 statistical analyses were undertaken in 'R' vs. 3.4.0. Source apportionment was modelled
260 using the Bayesian isotope mixing model of Stable Isotope Analysis in R (SIAR)' (Parnell
261 and Jackson, 2008, R Core Team, 2014).

262

263 **3. Results & Discussion**

264 3.1 Distinguishing between terrestrial and aquatic organic matter sources

265 Statistically significant differences (p<0.001) in the C/N ratio and bulk stable ¹³C and ¹⁵N
266 isotopic composition of terrestrial soils, river bed sediments and lake core sediments (Table
267 1), were determined. Woodland and river bed sediments exhibited the highest C/N ratios,

268 while the lowest C/N ratios were detected in arable and temporary grassland soils. The high
 269 C/N ratio in woodland soils and river sediments is characteristic of more recalcitrant OM
 270 sources such as wood, while the low C/N ratio is indicative of more decomposable OM with
 271 lower lignin content (Brady and Weil, 1999). Percentage C and % N were comparable
 272 between the woodland and grassland soils and lake sediments and differed from low % C and
 273 % N in cropland soils and river bed sediments, indicating fast OM turnover in cropland
 274 rotations and rapid loss of OM and inorganic N from river bed sediments to the downstream
 275 lake.

276 The highest bulk $\delta^{15}\text{N}$ values were detected in lake core sediments, followed by grassland and
 277 arable soils. Enriched $\delta^{15}\text{N}$ values in lake sediments may be due to several processes,
 278 including significant macrophyte or riparian-aquatic OM inputs (Fang et al., 2014), increased
 279 denitrification in anoxic lake bottom waters, and increased net primary production (Meyers,
 280 2003). Increased bulk $\delta^{15}\text{N}$ values on arable land may be indicative of both rapid turnover of
 281 OM and long-term application of manure (Glendell et al., 2014b). Bulk $\delta^{13}\text{C}$ values were
 282 relatively uniform between land uses, reflecting the predominance of C3 plants in the study
 283 catchment (Puttock et al., 2014). $\delta^{13}\text{C}$ values were enriched in arable soils and lake core
 284 sediments, with the former possibly reflecting periodic growing of maize, a C4 plant with a
 285 different photosynthetic pathway with natural abundance $\delta^{13}\text{C}$ values of $\sim -12\text{‰}$ (Beniston et
 286 al., 2015; Puttock et al., 2014) on arable land and the effect of in-lake organic matter
 287 production on lake bed sediments (Fang et al., 2014; Hamilton and Lewis, 1992). However, it
 288 is important to acknowledge that direct characterisation of the composition of autochthonous
 289 OM produced by aquatic plants in the lake ecosystem would allow a more conclusive
 290 interpretation of these findings.

291 Table 1 Elemental and isotopic composition (mean and SD in brackets) of all terrestrial soils,
 292 river bed sediment and lake core samples. Values followed by the same letter are not
 293 significantly different, while values followed by a different letter are significantly different
 294 ($p < 0.05$). N = number of replicates.

Landuse (N)	C/N	$\delta^{15}\text{N}$ (‰)	$\delta^{13}\text{C}$ (‰)	% C	% N
Arable (31)	8.99 (0.7) a	5.5 (0.8) a	-27.6 (0.4) a	2.92 (0.54)a	0.32 (0.05)a
Grass (14)	9.98 (0.8) b	5.6 (1.2) a, c	-28.2 (0.5) b	5.60 (1.21)b	0.56 (0.14)b
Ley (26)	9.23 (0.7) a	5.5 (0.9) a, c	-28.2 (0.40) b	3.60 (0.82)c	0.39 (0.07)c
Woodland (7)	12.84 (2.4) c	4.7 (1.5) a, c	-28.2 (0.3) b	8.06 (1.83)b	0.63 (0.14)bd
River (7)	12.20 (1.0) c	4.5 (1.1) a, d	-28.3 (0.2) b	2.34 (0.84)a	0.19 (0.06)a
Lake (27)	10.76 (0.6) c	6.3 (0.4) b	-27.6 (0.4) a	7.40 (1.08)b	0.69 (0.07)d

295

296 Concentrations of *n*-alkanes of chain lengths C_{15} - C_{33} in the six environments of interest
 297 showed a higher concentration of woody- (C_{27} - C_{29}) and grass- (C_{31}) derived OM input in lake
 298 sediments, as compared to terrestrial soils. Concurrently, shorter-chain *n*-alkanes indicative
 299 of aquatic macrophytes and lower plants such as mosses (C_{21} - C_{25}) (Meyers, 2003) were also
 300 apparent in lake sediments and in riparian woodland (Table 2). As expected, C_{31} chain
 301 lengths indicative of grasses (forage and cereals) (Eckmeier and Wiesenberg, 2009), were

302 more abundant in the soils of arable, temporary ley and permanent grassland land uses, while
 303 the C₂₇ chain-length *n*-alkanes, indicative of woody vegetation (Zech et al., 2009), were more
 304 abundant in woodland soils, river bed and lake core sediments.

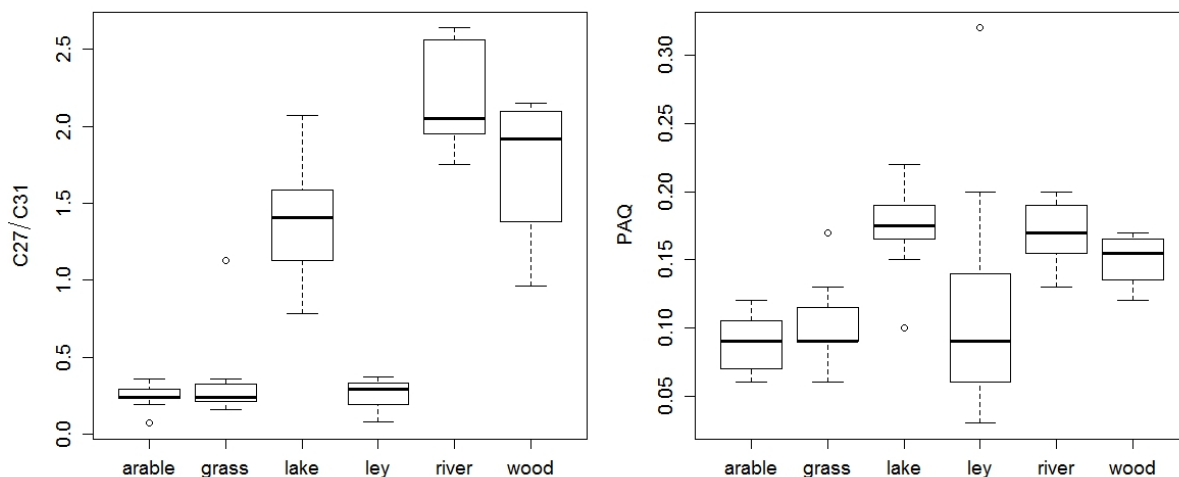
305 Table 2 *n*-alkane concentrations (µg g⁻¹ C) in soils and sediments from the six target
 306 environments. N – number of replicates.

N	n-alkane chain length concentration µg g ⁻¹ C									
	Mean (SD)									
Landuse	C15	C17	C19	C21	C23	C25	C27	C29	C31	C33
Arable (11)	0.16 (0.11)	0.22 (0.12)	n/a	0.65 (0.73)	0.22 (0.11)	0.40 (0.12)	0.93 (0.34)	2.68 (1.27)	3.86 (0.91)	1.99 (0.48)
Grass (7)	0.26 (0.18)	0.26 (0.17)	n/a	0.43 (0.17)	0.35 (0.20)	0.76 (0.33)	1.86 (1.32)	3.81 (1.32)	5.52 (1.25)	3.02 (1.02)
Ley (9)	0.25 (0.25)	0.32 (0.29)	n/a	0.92 (0.98)	0.46 (0.70)	0.83 (0.79)	1.29 (0.74)	3.10 (1.09)	4.79 (1.46)	2.22 (0.91)
Woodland (4)	0.11 (0.13)	0.22 (0.24)	n/a	0.94 (0.86)	0.92 (0.69)	2.98 (1.09)	12.93 (6.29)	13.89 (5.09)	7.40 (2.86)	4.40 (2.61)
River (7)	0.24 (0.20)	0.24 (0.21)	0.22 (0.09)	0.46 (0.40)	0.37 (0.20)	1.35 (0.51)	5.70 (2.11)	5.92 (2.24)	2.65 (1.04)	1.10 (0.52)
Lake (12)	0.26 (0.18)	1.28 (0.85)	0.96 (0.42)	0.96 (0.43)	1.90 (0.70)	4.17 (1.42)	16.45 (4.27)	16.62 (2.91)	12.08 (1.55)	4.93 (1.23)

307

308 Relative contribution of aquatic vs. terrestrial plants to OM was assessed with three
 309 indicators, C₂₇/C₃₁ ratios, PAQ and TAR. As expected highest C₂₇/C₃₁ ratios, indicative of
 310 woody sources were found in the woodland soil samples, while low C₂₇/C₃₁ ratios in the
 311 remaining terrestrial soils were indicative of OM origin from grassland vegetation (including
 312 cereal crops and forage grass). The river bed sediments were also characterised by higher
 313 C₂₇/C₃₁ ratios, indicating predominant sediment input from soils under woody vegetation in
 314 the well-connected wooded riparian buffer strip (Fig. 2a). The lake sediments appear to be
 315 intermediary between these land uses, indicating OM contribution from both woody and
 316 grass vegetation, which may be related to OM transport during high-flow events. During
 317 rainfall events, the less connected arable/grassland sources may make a greater contribution
 318 to OM transport, which is likely to be directly routed to the lake, without being deposited in
 319 river bed sediments.

320 Higher median PAQ ratios of > 0.15 in the lake, river and riparian woodland environments
 321 were indicative of emergent macrophyte origin, while the lower median ratios <0.1 were
 322 indicative of terrestrial plants (Fig. 2b). The higher PAQ ratios in the riparian woodland may
 323 reflect a contribution from lower plants including mosses, which were abundant on the
 324 ground of this wet woodland. Still there remains a large unexplained variability of observed
 325 PAQ, particularly in the grass ley.



326

327 Fig. 2 Box plots of *n*-alkane ratios a) C₂₇/C₃₁ indicating OM prevalence from woody vs. grass
 328 dominated sources b) PAQ indicating contribution of OM from aquatic/lower plant vs.
 329 terrestrial vegetation. The bottom and top of the box refer to the 25th and 75th percentile, the
 330 bold line near the middle to the 50th percentile (the median) and whiskers following the
 331 default setting of R, respectively.

332

333 While single tracers and ratios presented above cannot unravel contribution of several sources
 334 on their own, a global assessment with a Principal Component Analysis (PCA) was
 335 undertaken. PCA revealed that a combined *n*-alkane, elemental and stable ¹³C and ¹⁵N isotopic
 336 signatures provide a clear separation in sediment fingerprint composition (Fig. 3). The PCA
 337 axis 1 can be interpreted as a gradient between grassland and arable land uses with higher %
 338 C₃₁ *n*-alkane signature (indicating grass-derived OM) vs. riparian woodland and aquatic
 339 environments with a higher % C₂₇, higher C₂₇:C₃₁ and C/N ratios (indicating wood-derived
 340 OM sources), lower % C₂₉ (indicating lower plants in the woodland ground vegetation) and
 341 higher PAQ (Tables 2-4, Fig. 3a). The PCA axis 2 can be interpreted as a gradient between
 342 river bed sediments and lake core sediments, with the latter supporting higher δ¹³C and δ¹⁵N
 343 isotopic signatures and higher % C and % N content (Tables 2-4, Fig. 3a) and indicating
 344 different sediment dynamics in the two aquatic environments. This is also reflected in Fig 3b,
 345 which shows a clear distinction in sediment composition between lake and river bed
 346 sediments and woodland, permanent grassland and cropland sources. However, PCA could
 347 not distinguish soils from temporary grassland (ley) and arable land, presumably because
 348 these two land uses are subject to regular rotations. While other researchers have also found it
 349 possible to distinguish between permanent grassland and woodland sediment and OM
 350 sources, they were unable to distinguish between arable land use and permanent grassland,
 351 based on the use of biomarkers alone (Alewell et al., 2015). In this study, the combined use
 352 of biomarkers and elements (% C, % N, C/N ratio) allowed us to distinguish between these
 353 two land uses as the % N and % C as well as C/N ratio are all higher in grassland soils than in
 354 arable and temporary grass ley (Tables 3-4), thus acting as further informative tracers in
 355 addition to *n*-alkanes.

356 Table 3 Biogeochemical values (mean and SD) of the 50 source soils, river bed sediments
 357 and lake core samples included in the PCA analysis. N = number of replicates.

Land use (N)	C ₂₇ :C ₃₁	PAQ	% C ₂₇	% C ₂₉	% C ₃₁	% N	δ ¹⁵ N (‰)	% C	C/N	δ ¹³ C (‰)
Mean (SD)										
Arable (11)	0.25 (0.08)	0.09 (0.02)	0.13 (0.04)	0.35 (0.06)	0.52 (0.06)	0.33 (0.05)	5.3 (1.03)	3.05 (0.64)	9.32 (0.97)	-27.6 (0.42)
Grass (7)	0.37 (0.34)	0.10 (0.04)	0.16 (0.07)	0.33 (0.04)	0.51 (0.11)	0.52 (0.10)	5.2 (1.21)	5.40 (1.08)	10.39 (0.86)	-28.0 (0.57)
Ley (9)	0.26 (0.10)	0.12 (0.09)	0.13 (0.04)	0.34 (0.01)	0.53 (0.04)	0.40 (0.08)	5.2 (0.63)	3.77 (1.07)	9.21 (0.86)	-28.2 (0.33)
Woodland (4)	1.74 (0.54)	0.15 (0.02)	0.37 (0.07)	0.41 (0.05)	0.22 (0.04)	0.62 (0.16)	4.7 (1.97)	7.80 (2.29)	12.67 (3.23)	-28.3 (0.31)
River (7)	2.21 (0.37)	0.17 (0.03)	0.40 (0.03)	0.41 (0.02)	0.19 (0.02)	0.19 (0.06)	4.5 (1.06)	2.34 (0.84)	12.20 (1.01)	-28.3 (0.24)
Lake (12)	1.37 (0.37)	0.17 (0.03)	0.36 (0.05)	0.37 (0.01)	0.27 (0.05)	0.70 (0.07)	6.4 (0.31)	7.61 (0.95)	10.91 (0.46)	-27.7 (0.41)

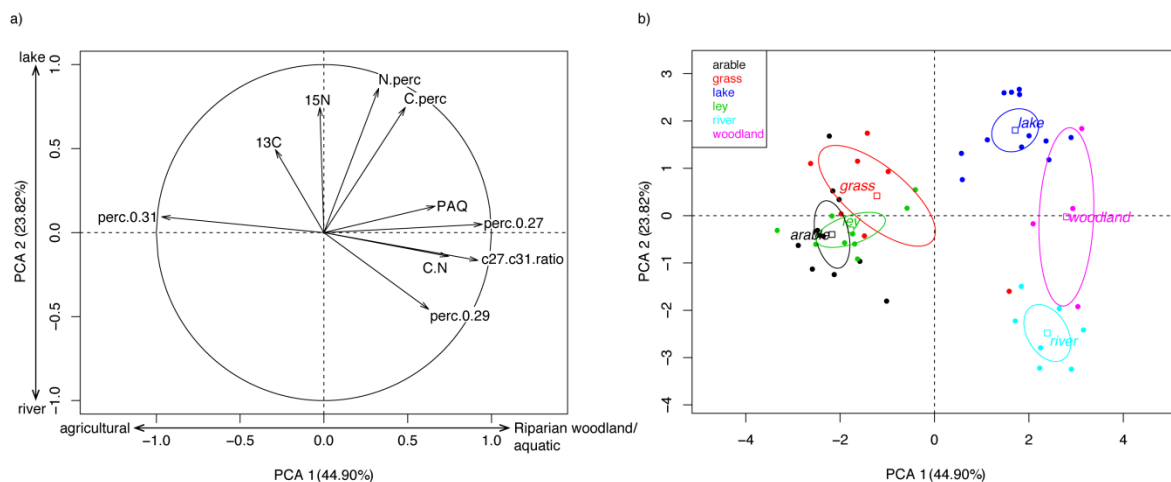
358

359 Table 4 Loading scores of ten biochemical tracers, initial eigenvalues and % total variance
 360 accounted for by the first three PCA axes with eigenvalues >1. Loading scores >0.3 were
 361 used in the interpretation of axes.

	axis 1	axis 2	axis 3
%N	0.33	0.86	-0.34
delta 15N		0.74	0.48
%C	0.49	0.75	-0.45
C/N	0.74		-0.38
delta 13C		0.49	0.34
C27/C31	0.92		
PAQ	0.66		0.35
C27	0.95		
C29	0.63	-0.46	

C31	-0.97		
Arable	-2.17	-0.40	
Grass	-1.22	0.42	-0.81
Lake	1.71	1.80	
Ley	-1.77		
River	2.39	-2.48	0.91
woodland	2.79		-1.28
Eigenvalues	4.49	2.38	1.06
% of variance	44.90	23.82	10.65
Cumulative % of variance	44.90	68.71	79.36

362



363

364

365

366

Fig. 3 Two-dimensional plot of a) variable distribution along the first two PCA ordination axes b) sampling site loading scores on the first two PCA axes and 95% confidence ellipses around the categories of land use.

367

3.2 Spatial variability of land use and provenance of OM in river bed sediments

368

369

370

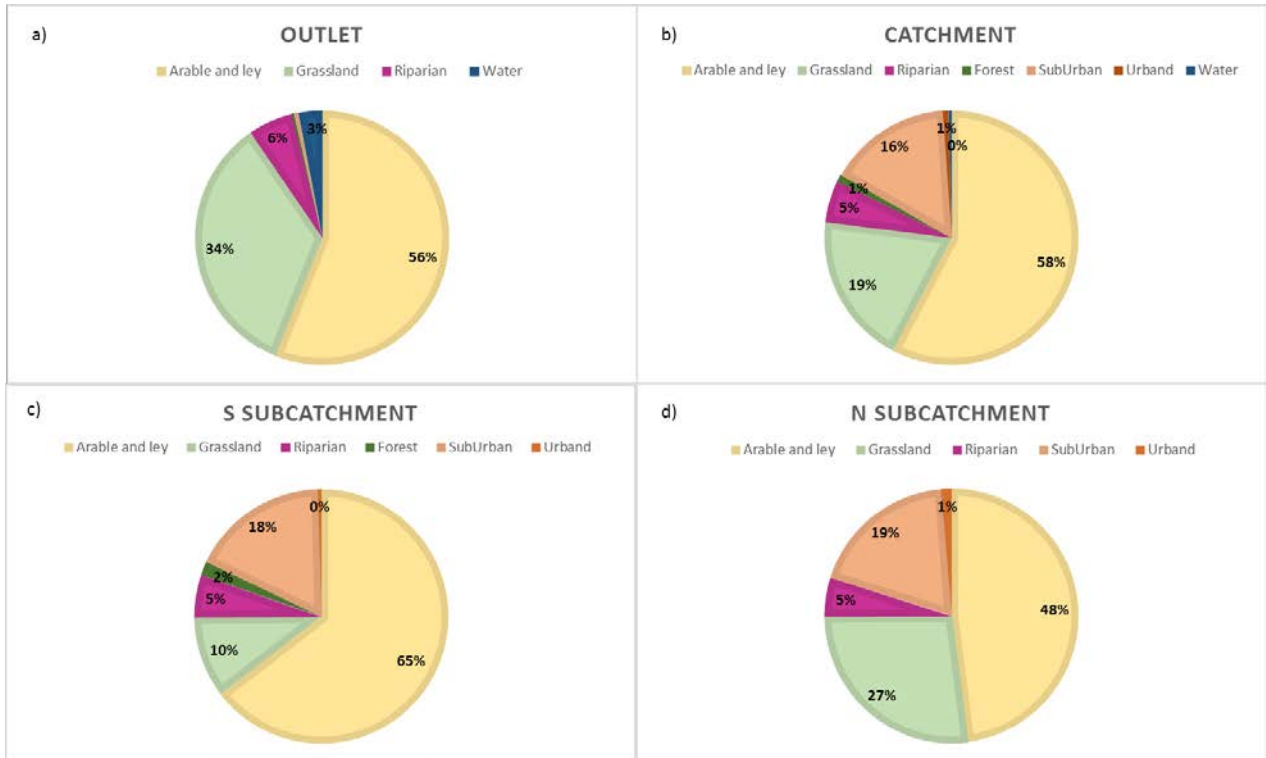
371

372

Spatial patterns of OM provenance in relation to land use were examined at each river bed sediment sampling location (“upstream”, midstream”, “downstream” and “outlet”) in the two subcatchments (S and N) (Figs. 1, 4, 5). Organic matter fingerprinting properties reflected some subtle differences in land used between the two subcatchments. While both the S and N subcatchments were characterized by ca. 75 % agricultural land use, 20 % sub-urban land

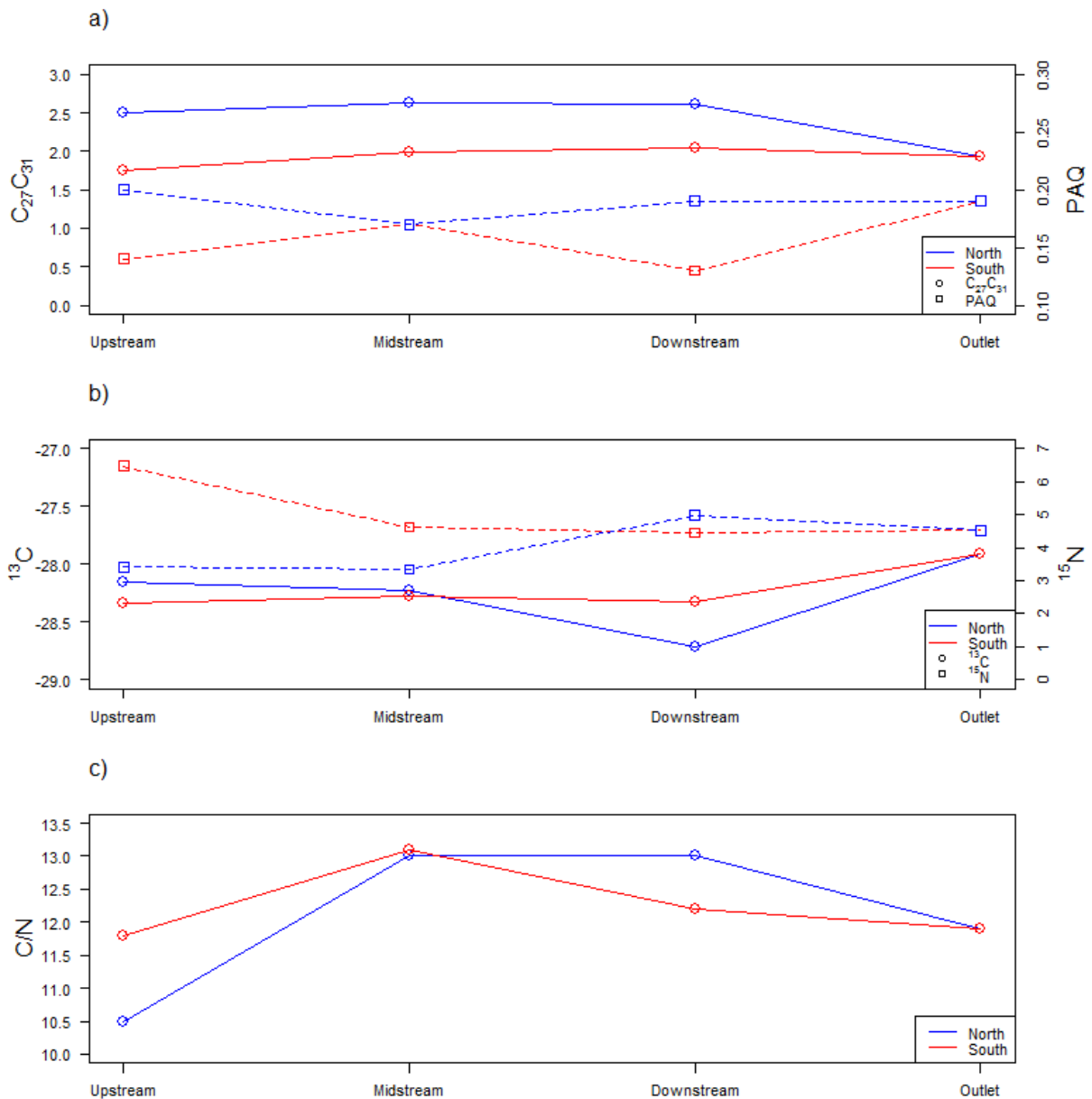
373 use and 5 % of riparian vegetation in the riparian corridor, the S subcatchment supported a
 374 higher arable and ley vs. permanent grassland ratio (65 % to 10 %, respectively) than the N
 375 subcatchment (48 % to 19 %, respectively) (Fig. 4).

376



377

378 Fig. 4 Proportion of different land uses a) at the outlet sampling location b) the whole study
 379 catchment c) Southern subcatchment and d) Northern subcatchment.



380

381 Fig. 5 Spatial variability of a) *n*-alkane proxies b) stable isotopes and c) C/N ratio in a
 382 downstream direction in the two subcatchments.

383 This was reflected in river bed OM properties, which had lower C_{27}/C_{31} ratios than in the N
 384 subcatchment, with the upstream location supporting the lowest C_{27}/C_{31} *n*-alkane value of
 385 1.75 overall (Fig 5a), likely due to a higher proportion of arable and ley land use in this
 386 subcatchment (Fig 4c) leading to higher soil erosion rates (Turnage et al., 1997). The
 387 observed higher $\delta^{15}N$ values at the most upstream location (ca.+7 ‰, Fig 5b) may also be
 388 associated with a higher application of farmyard manure and slurry to arable land and ley
 389 (Bol et al., 2005; Senbayram et al., 2008). Conversely, the higher C_{27}/C_{31} ratio in the N
 390 subcatchment and the lack of upstream forested areas indicate a higher contribution of OM
 391 from wooded vegetation in the riparian zone, as well as a potential buffering of terrestrial OM
 392 fluxes from agricultural soils in the vegetated river corridor. Higher PAQ ratios in the N
 393 subcatchment, indicating a relatively higher contribution of mosses and macrophytes derived

394 OM, also point towards a greater influence of the riparian zone on lateral C fluxes as
395 compared to the S stream (Fig. 5a).

396 Higher C_{27}/C_{31} and C/N ratios (Fig. 5a & 5c) at the midstream and downstream locations in
397 both subcatchments indicated an increased contribution of OM from woody vegetation to
398 river bed sediments in these river reaches. The C_{27}/C_{31} *n*-alkane ratio at the joint catchment
399 outlet was lower than in the N subcatchment but similar to the ratios found in the S sub-
400 catchment (Fig. 5a), indicating mixing of OM from the two tributaries as well as input from
401 permanent grasslands situated on the steep slopes in the lower reaches of the river corridor.

402

403 3.3 Impact of land use on sediment and C accumulation in lake bed sediments

404

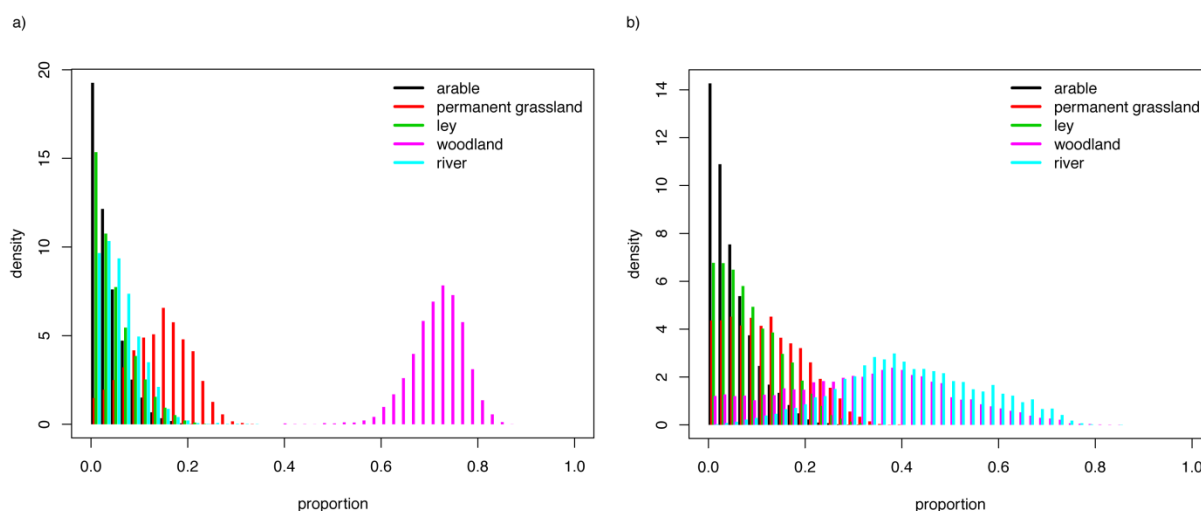
405 Source apportionment modelling of the lake core sediments has shown different results,
406 depending on the composition of the fingerprint signatures. Currently, there is a lack of
407 consensus within the sediment fingerprinting community on the most appropriate selection of
408 fingerprint tracers (Sherriff et al., 2015; Zhang and Liu, 2016). Therefore, in this study, we
409 firstly included all tracers used in the PCA in the source apportionment analysis (Fig. 6a),
410 followed by just those tracers that encompassed the range of values represented in the
411 mixture (and therefore deemed as conservative) (Fig. 6b). The second approach included
412 $C_{27}:C_{31}$ ratio, % C_{27} , % C_{29} and % C_{31} . As such we had 4 tracers (n) to apportion the
413 contribution of five sources (n+1). In both cases, organic C from riparian woodland was a
414 major contributor to the lake sediments. In the second scenario, river bed sediments appeared
415 to make the second largest contribution to lake core sediments over the past 60 years (Fig.
416 6b). However, as river bed sediments are also dominated by woody vegetation, as shown in
417 Fig. 2a above, they can be considered 'equal to' woodland signatures in this apportionment
418 model, due to the restricted number of very selective tracers. However, in both modelling
419 outcomes, the important contribution of organic matter from permanent grassland, which
420 occupies the steep slopes surrounding the lake, is very apparent (Fig. 6a).

421

422 Zhang and Liu (2016) also found that tracer selection greatly impacted the estimated source
423 contributions, due to a number of potential reasons, including i) tracer conflicts ii) tracer
424 measurement error and iii) differences in tracer conservativeness. Therefore, they proposed to
425 use multiple fingerprints to derive 'average' estimated source contribution proportions,
426 instead of just a single fingerprint set. While different sediment contributions can be obtained
427 with different fingerprint selection, recent studies (Palazón et al., 2015; Sherriff et al., 2015)
428 have found that inclusion of more tracers improved the source apportionment results. In this
429 study, modelling results based on the full set of tracers (Fig. 6a) allowed a finer distinction
430 between contributing land uses.

431

432 Conversely to lake core sediments, it was not possible to model the source apportionment of
 433 river bed sediments satisfactorily as all potential tracers in bed sediments appeared to be
 434 outside the range of the potential sources. This apparently ‘missing source’ opens new lines
 435 of enquiry for future research. At present we hypothesise that the ‘missing source’ may either
 436 be due to the contribution of petrogenic C originating from the underlying bedrock (Galy et
 437 al., 2015) or that the *n*-alkane signatures have been altered by autochthonous in-stream
 438 production of OM (e.g. from algae) and by in-stream biological processing of river bed
 439 sediments (Chen et al., 2016).



1
 2 Fig. 6 Probability density function of sediment source apportionment sources from different
 3 land uses using a) all available tracers b) only tracers that encompass the full range of values
 4 present in the mixture for the application of the mixing model SIAR.

5

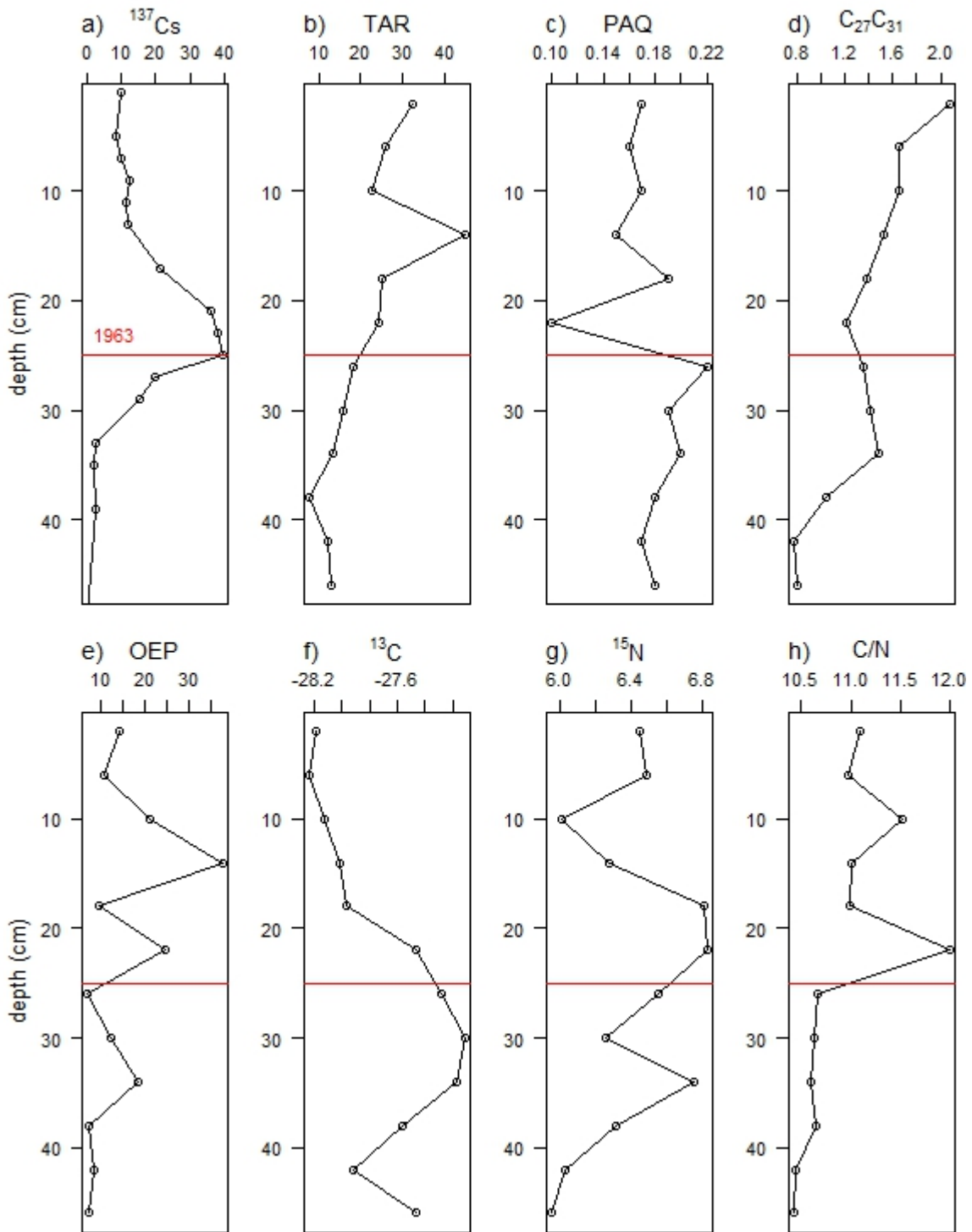
6 3.4 Understanding the temporal variability of lateral C fluxes from land to water in
 7 relation to land use change

8

9 Caesium-137 (^{137}Cs) activity was used to get an approximate dating profile for the lake bed
 10 sediment core (Fig. 7a). The depth distribution of ^{137}Cs within the core was analysed and the
 11 horizon containing peak activity was identified at 26 cm and was assumed to be associated
 12 with the peak in bomb derived ^{137}Cs fallout attributed to 1963. The offset of bomb testing in
 13 1952 was assumed to be associated with lake core depth at 34 cm.

14

15



16

17 Figure 7 Lake core profiles showing a) ^{137}Cs activity used to date the lake sediment core and
 18 interpret the observed changes in sediment composition over time b-h) sediment
 19 fingerprinting characteristics with depth.

20

21

22 The combined use of *n*-alkane ratios and stable isotope signatures shows a variable
23 contribution of terrestrial vs. aquatic sources to sediment accumulation in individual lake core
24 increments over the past 60 years (Fig. 7b-h). The TAR ratio (Fig. 7b) indicates an
25 increasing contribution of terrestrial-derived OM to the lake sediments, while the increasing
26 C₂₇/C₃₁ ratio (Fig. 7d) indicates an increase of woody vegetation contribution over the same
27 time period. This is corroborated by the fact that the signal from PAQ *n*-alkane proxy lies
28 within the range of 0.01 to 0.23 (Fig. 7c), deemed indicative of terrestrial plants (Silliman and
29 Schelske, 2003) and suggesting mainly allochthonous source of sedimentary OM. The
30 depletion in $\delta^{13}\text{C}$ values with depth (Fig. 7f) may also indicate an increasing input of
31 isotopically lighter soil-derived dissolved inorganic C (Meyers, 2003) – and thus increasing
32 terrestrial input of C from soil erosion. However, it may also be due to the preferential loss of
33 the light isotope (^{12}C) through microbial respiration over time (Beniston, et al. 2014). In any
34 case correlation between OEP and TAR ratios ($p < 0.001$, $R^2 = 0.53$) suggests reduced OM
35 decomposition associated with increasing terrestrial contribution of OM over the past 60
36 years (Zech et al., 2013), which may be linked to a higher C/N ratio – and therefore lower
37 bioavailability of woodland and grassland derived OM.

38 While increased $\delta^{15}\text{N}$ enrichment (Fig. 7g) may be indicative of increased net primary
39 production associated with the reported eutrophication of Loe Pool since the 1960s (Dinsdale,
40 2009), it is not likely to be due to an increase in N fixing cyanobacteria, which directly fix
41 atmospheric N_2 and therefore lead to lower $\delta^{15}\text{N}$ signatures in sediments and would be
42 expected to lead to an increased $\delta^{13}\text{C}$ signature due to enhanced NPP (Meyers and Lallier-
43 Vergès, 1999; Meyers, 2003). In addition, increased $\delta^{15}\text{N}$ enrichment may be associated with
44 enhanced denitrification (preferential loss of the light ^{14}N isotope) in anoxic lake bottom
45 waters (Meyers, 2003) or with higher natural abundance ^{15}N -enriched signatures originating
46 from faeces from farmyard manures (Senbayram et al. 2008) and septic tanks (Collins, et al.
47 2013; 2014).

48 However, it is acknowledged that $\delta^{13}\text{C}$ enrichment and C/N ratios are not always indicative of
49 sources as they can be affected by degradation (Ranjan et al., 2015). Laceby et al. (2015)
50 found that while $\delta^{15}\text{N}$ bulk isotopic signatures of sediment sources exhibited non-
51 conservative behaviour, $\delta^{13}\text{C}$ signatures appeared to be more stable. Fang et al. (2014)
52 observed that significant macrophyte or riparian-aquatic OM inputs may lead to higher $\delta^{15}\text{N}$
53 and $\delta^{13}\text{C}$ values in lake sediments, thus confounding our ability to distinguish between the
54 terrestrial and aquatic input of OM on the basis of bulk stable ^{13}C and ^{15}N isotopic signatures
55 alone. Therefore, compound-specific stable ^{13}C isotope (CSSIA) signatures of plant-derived
56 biomarkers are currently explored as more suitable tracers, as the isotopic signatures of
57 individual molecules are likely to be more conservative than bulk stable isotopes alone (Fang
58 et al., 2014; Tao et al., 2016).

59 In this study, the combined use of *n*-alkanes and bulk stable ^{13}C and ^{15}N isotopes detected
60 increased terrestrial input of sediment and increased lake eutrophication over the past 60
61 years, with terrestrial grass and woody plant-derived *n*-alkanes being more indicative of OM
62 sources, and stable ^{13}C and ^{15}N isotopes being more indicative of in-stream and in-lake

63 processes. The application of compound-specific stable isotope $\delta^{13}\text{C}$ and $\delta^2\text{H}$ signatures of
64 specific *n*-alkane molecules, as opposed to a separate use of *n*-alkane chain length and bulk
65 stable ^{13}C and ^{15}N isotopes, may help to better differential between aquatic and terrestrial
66 plant origin of organic matter in future work (Cooper et al., 2015) and thus quantify the
67 autochthonous vs. allochthonous organic matter contribution. Further improvements may be
68 obtained by multi-molecular investigations using simultaneous application of different
69 biomarkers and ^{14}C isotopes to constrain the transfer of C from land to the ocean (Feng et al.,
70 2015).

71 The ability to discern OM contribution to aquatic environments from different land uses
72 found in this study, provides an important new tool for the understanding of OM fluxes from
73 land to water at catchment scales. Wohl et al. (2017) proposed a revised paradigm for the
74 understanding of the role of rivers in the transport and processing of terrestrial C, whereby
75 the active river channel and the riparian zone function as one coupled system – a *river*
76 *corridor*, in which riparian areas act ‘as biogeochemical reactors that facilitate the speciation,
77 transformation, and opportunities for both long-term storage of carbon and mineralization to
78 the atmosphere’. Wohl et al. (2017) posit that while alteration of riparian zone is the most
79 significant and most highly altered aspect of lateral C dynamics, very little is known about
80 the sources and quantities of different kinds of OM stored within river corridors and how C
81 inputs have varied over decadal and millennial timescales as a results of human activities. In
82 this study, we also found very close coupling between the aquatic sediments and the riparian
83 zone and our ability to discern between these sources provides a new opportunity to quantify
84 the lateral C fluxes at catchment scales. Coupling the fingerprinting approach explored in this
85 paper with future modelling of soil erosion rates is a promising new tool for quantifying these
86 lateral C fluxes at a range of scales.

87

88 **4. Conclusions**

89 This pilot study tested a new approach to quantify the lateral fluxes of OM from the terrestrial
90 to aquatic environments at a catchment scale. Here we evaluated the combined use of the
91 abundance and ratios of conservative plant-derived biomarkers *n*-alkanes and bulk stable
92 isotopes to distinguish between OM and sediment provenance from different environments.
93 While it was possible to distinguish between arable and temporary grassland, permanent
94 grassland, woodland, river and lake environments, it was not possible to distinguish between
95 arable land and temporary grassland, as these two land uses are part of regular rotations.
96 However, the combined use of biomarkers and stable isotopes allowed us to distinguish
97 between sediment sources from arable and permanent grassland land uses, which has not
98 been previously possible with the use of biomarkers alone. Furthermore, the combined use of
99 biomarkers and stable isotopes enabled us to detect the observed change in the lake trophic
100 status over the past 60 years and attribute this to changing land use, resulting in enhanced
101 sedimentation and nutrient flux from the terrestrial to the aquatic environments. These
102 enhanced lateral OM fluxes can be linked to agricultural intensification, resulting in higher
103 soil erosion rates, over the same period. Moreover, we detected an increased contribution of

104 woody vegetation to the OM provenance over time, most likely indicating an increase in the
105 woody vegetation covering the near-stream riparian corridor. The new fingerprinting
106 approach successfully discriminated between terrestrial *vs.* aquatic C sources and when
107 coupled with quantitative estimates of soil erosion rates, it shows to be a promising new tool
108 for the understanding of lateral C fluxes from land to water at a range of scales. The close
109 coupling between OM provenance and riparian land use observed in this study underlines the
110 importance of the riparian zone for lateral C transfers and thus support the new holistic
111 conceptualization of ‘river corridors’ as critical zones linking the terrestrial and aquatic C
112 (Wohl et al., 2017).

113

114 **Acknowledgements** This work was supported by the University of Exeter Strategic Science
115 Development Fund and UK Natural Environment Research Council GW4+ Research
116 Experience Placement Scheme. We would like to thank Iain Hartley and Gabriel Yvon-
117 Durocher of the University of Exeter for helpful scientific discussions at the project inception
118 and to two anonymous reviewers for their constructive comments that greatly helped to
119 improve our manuscript

120

121 **References**

- 122 Adhikari, K., Hartemink, A.E., 2016. Linking soils to ecosystem services - A global review.
123 *Geoderma* 262, 101–111. doi:10.1016/j.geoderma.2015.08.009
- 124 Alewell, C., Egli, M., Meusburger, K., 2015. An attempt to estimate tolerable soil erosion
125 rates by matching soil formation with denudation in Alpine grasslands. *J. Soils*
126 *Sediments* 1–17. doi:10.1007/s11368-014-0920-6
- 127 Alewell, C., Birkholz, A., Meusburger, K., Schindler Wildhaber, Y., Mabit, L., 2016.
128 Quantitative sediment source attribution with compound-specific isotope analysis in a
129 C3 plant-dominated catchment (central Switzerland). *Biogeosciences* 13, 1587–1596.
130 doi:10.5194/bg-13-1587-2016
- 131 Alewell, C., Birkholz, A., Meusburger, K., Schindler Wildhaber, Y., Mabit, L., 2015.
132 Sediment source attribution from multiple land use systems with CSIA. *Biogeosciences*
133 *Discuss.* 12, 14245–14269. doi:10.5194/bgd-12-14245-2015
- 134 Amundson, R., Berhe, A.A., Hopmans, J.W., Olson, C., Sztein, A.E., Sparks, D.L., 2015.
135 Soil science. Soil and human security in the 21st century. *Science* 348, 1261071.
136 doi:10.1126/science.1261071
- 137 Aufdenkampe, A.K., Mayorga, E., Raymond, P.A., Melack, J.M., Doney, S.C., Alin, S.R.,
138 Aalto, R.E., Yoo, K., 2011. Riverine coupling of biogeochemical cycles between land,
139 oceans, and atmosphere. *Front. Ecol. Environ.* 9, 53–60. doi:10.1890/100014
- 140 Battin, T.J., Luysaert, S., Kaplan, L. a., Aufdenkampe, A.K., Richter, A., Tranvik, L.J.,
141 2009. The boundless carbon cycle. *Nat. Geosci.* 2, 598–600. doi:10.1038/ngeo618
- 142 Beniston, J.W., DuPont, S.T., Glover, J.D., Lal, R., Dungait, J.A.J., 2014. Soil organic carbon

- 143 dynamics 75 years after land-use change in perennial grassland and annual wheat
144 agricultural systems. *Biogeochemistry* 120, 37–49.
- 145 Beniston, J.W., Shipitalo, M.J., Lal, R., Dayton, E.A., Hopkins, D.W., Jones, F., Joynes, A.,
146 Dungait, J.A.J., 2015. Carbon and macronutrient losses during accelerated erosion under
147 different tillage and residue management. *Eur. J. Soil Sci.* 66, 218–225.
- 148 Bilotta, G.S., Brazier, R.E., 2008. Understanding the influence of suspended solids on water
149 quality and aquatic biota. *Water Res.* 42, 2849–2861. doi:10.1016/j.watres.2008.03.018
- 150 Blake, W.H., Ficken, K.J., Taylor, P., Russell, M.A., Walling, D.E., 2012. Tracing crop-
151 specific sediment sources in agricultural catchments. *Geomorphology* 139–140, 322–
152 329. doi:10.1016/j.geomorph.2011.10.036
- 153 Bol, R., Eriksen, J., Smith, P., Garnett, M.H., Coleman, K., Christensen, B.T., 2005. The
154 natural abundance of ¹³C, ¹⁵N, ³⁴S and ¹⁴C in archived (1923–2000) plant and soil
155 samples from the Askov long-term experiments on animal manure and mineral fertilizer.
156 *Rapid Commun. Mass Spectrom.* 19, 3216–3226.
- 157 Brady, N.C., Weil, R.R., 1999. *The Nature and Properties of Soils*. Prentice Hall, Upper
158 Saddle River, New Jersey.
- 159 Brevik, E.C., Cerdà, a., Mataix-Solera, J., Pereg, L., Quinton, J.N., Six, J., Van Oost, K.,
160 2015. The interdisciplinary nature of *SOIL*. *Soil* 1, 117–129. doi:10.5194/soil-1-117-
161 2015
- 162 Chen, F., Fang, N., Shi, Z., 2016. Using biomarkers as fingerprint properties to identify
163 sediment sources in a small catchment. *Sci. Total Environ.* 557–558, 123–133.
164 doi:10.1016/j.scitotenv.2016.03.028
- 165 Chen, F.X., Fang, N.F., Wang, Y.X., Tong, L.S., Shi, Z.H., 2017. Biomarkers in sedimentary
166 sequences: Indicators to track sediment sources over decadal timescales.
167 *Geomorphology* 278, 1–11. doi:10.1016/j.geomorph.2016.10.027
- 168 Cole, J.J., Prairie, Y.T., Caraco, N.F., McDowell, W.H., Tranvik, L.J., Striegl, R.G., Duarte,
169 C.M., Kortelainen, P., Downing, J.A., Middelburg, J.J., Melack, J., 2007. Plumbing the
170 global carbon cycle: Integrating inland waters into the terrestrial carbon budget.
171 *Ecosystems* 10, 171–184. doi:10.1007/s10021-006-9013-8
- 172 Collins, A.L., Williams, L.J., Zhang, Y.S., Marius, M., Dungait, J.A.J., Smallman, D.J.,
173 Dixon, E.R., Stringfellow, A., Sear, D.A., Jones, J.I., Naden, P.S., 2013. Catchment
174 source contributions to the sediment-bound organic matter degrading salmonid
175 spawning gravels in a lowland river, southern England. *Sci. Total Environ.* 456, 181–
176 195.
- 177 Collins, A.L., Williams, L.J., Zhang, Y.S., Marius, M., Dungait, J.A.J., Smallman, D.J.,
178 Dixon, E.R., Stringfellow, A., Sear, D.A., Jones, J.I., Naden, P.S., Collins, A.L.,
179 Williams, L.J., Zhang, Y.S., Marius, M., Dungait, J.A.J., Smallman, D.J., Dixon, E.R.,
180 Stringfellow, A., Sear, D.A., Jones, J.I., Naden, P.S., 2014. Sources of sediment-bound
181 organic matter infiltrating spawning gravels during the incubation and emergence life
182 stages of salmonids. *Agric. Ecosyst. Environ.* 196, 76–93.
183 doi:10.1016/j.agee.2014.06.018

- 184 Cooper, R.J., Pedentchouk, N., Hiscock, K.M., Disdle, P., Krueger, T., Rawlins, B.G., 2015.
 185 Apportioning sources of organic matter in streambed sediments: An integrated
 186 molecular and compound-specific stable isotope approach. *Sci. Total Environ.* 520, 187–
 187 197. doi:10.1016/j.scitotenv.2015.03.058
- 188 Dinsdale, J., 2009. Loe Pool Catchment Management Project 2009 Review.
- 189 Eckmeier, E., Wiesenberg, G.L.B., 2009. Short-chain n-alkanes (C16-20) in ancient soil are
 190 useful molecular markers for prehistoric biomass burning. *J. Archaeol. Sci.* 36, 1590–
 191 1596. doi:10.1016/j.jas.2009.03.021
- 192 Eglinton, G., Gonzalez, A.G., Hamilton, R.J., Raphael, R.A., 1962. Hydrocarbon constituents
 193 of the wax coatings of plant leaves: A taxonomic survey. *Phytochemistry* 1, 89–102.
- 194 Fang, J., Wu, F., Xiong, Y., Li, F., Du, X., An, D., Wang, L., 2014. Source characterization
 195 of sedimentary organic matter using molecular and stable carbon isotopic composition
 196 of n-alkanes and fatty acids in sediment core from Lake Dianchi, China. *Sci. Total*
 197 *Environ.* 473–474, 410–21. doi:10.1016/j.scitotenv.2013.10.066
- 198 Feng, X., Gustafsson, Holmes, R.M., Vonk, J.E., Van Dongen, B.E., Semiletov, I.P.,
 199 Dudarev, O. V., Yunker, M.B., MacDonald, R.W., Montluçon, D.B., Eglinton, T.I.,
 200 2015. Multi-molecular tracers of terrestrial carbon transfer across the pan-Arctic:
 201 Comparison of hydrolyzable components with plant wax lipids and lignin phenols.
 202 *Biogeosciences* 12, 4841–4860. doi:10.5194/bg-12-4841-2015
- 203 Ficken, K.J., Li, B., Swain, D.L., Eglinton, G., 2000. An n-alkane proxy for the sedimentary
 204 input of submerged/floating freshwater aquatic macrophytes. *Org. Geochem.* 31, 745–
 205 749. doi:10.1016/S0146-6380(00)00081-4
- 206 Galy, V., Eglinton, T., France-Lanord, C., Sylva, S., 2011. The provenance of vegetation and
 207 environmental signatures encoded in vascular plant biomarkers carried by the Ganges-
 208 Brahmaputra rivers. *Earth Planet. Sci. Lett.* 304, 1–12. doi:10.1016/j.epsl.2011.02.003
- 209 Galy, V., Peucker-Ehrenbrink, B., Eglinton, T., 2015. Global carbon export from the
 210 terrestrial biosphere controlled by erosion. *Nature* 521, 204–207.
 211 doi:10.1038/nature14400
- 212 Glendell, M., Brazier, R.E., 2014. Accelerated export of sediment and carbon from a
 213 landscape under intensive agriculture. *Sci. Total Environ.* 476–477, 643–656.
 214 doi:10.1016/j.scitotenv.2014.01.057
- 215 Glendell, M., Extence, C., Chadd, R., Brazier, R.E., 2014a. Testing the pressure-specific
 216 invertebrate index (PSI) as a tool for determining ecologically relevant targets for
 217 reducing sedimentation in streams. *Freshw. Biol.* 59, 353–367. doi:10.1111/fwb.12269
- 218 Glendell, M., Granger, S.J., Bol, R., Brazier, R.E., 2014b. Quantifying the spatial variability
 219 of soil physical and chemical properties in relation to mitigation of diffuse water
 220 pollution. *Geoderma* 214–215, 25–41.
- 221 Graeber, D., Goyenola, G., Meerhoff, M., Zwirnmann, E., Ovesen, N.B.B., Glendell, M.,
 222 Gelbrecht, J., Teixeira de Mello, F., González-Bergonzoni, I., Jeppesen, E., Kronvang,
 223 B., 2015. Interacting effects of climate and agriculture on fluvial DOM in temperate and
 224 subtropical catchments. *Hydrol. Earth Syst. Sci.* 19, 2377–2394. doi:10.5194/hess-19-

- 225 2377-2015
- 226 Guzman, G., Quinton, J.N., Nearing, M.A., Mabit, L., Gómez, J.A., 2013. Sediment tracers in
227 water erosion studies: Current approaches and challenges. *J. Soils Sediments* 13, 816–
228 833. doi:10.1007/s11368-013-0659-5
- 229 Hamilton, S.K., Lewis, W.M., 1992. Stable carbon and nitrogen isotopes in algae and detritus
230 from the Orinoco River floodplain, Venezuela. *Geochim. Cosmochim. Acta* 56, 4237–
231 4246.
- 232 Laceby, J.P., Olley, J., Pietsch, T.J., Sheldon, F., Bunn, S.E., 2015. Identifying subsoil
233 sediment sources with carbon and nitrogen stable isotope ratios. *Hydrol. Process.* 29,
234 1956–1971. doi:10.1002/hyp.10311
- 235 Lauerwald, R., Laruelle, G.G., Hartmann, J., Ciais, P., Regnier, P.A.G., 2015. Global
236 Biogeochemical Cycles 534–554. doi:10.1002/2014GB004941.Received
- 237 Li, M., Peng, C., Wang, M., Xue, W., Zhang, K., Wang, K., Shi, G., Zhu, Q., 2017. The
238 carbon flux of global rivers: A re-evaluation of amount and spatial patterns. *Ecol. Indic.*
239 80, 40–51. doi:10.1016/j.ecolind.2017.04.049
- 240 Ludwig, W., P. Amiotte-Suchet, J.L. Probst, F.G. Hall, G.J. Collatz, B.W. Meeson, S.O. Los,
241 E.Brown De Colstoun, and D.R.L., 2011. ISLSCP II Global River Fluxes of Carbon and
242 Sediments to the Oceans.
- 243 Maavara, T., Lauerwald, R., Regnier, P., Van Cappellen, P., 2017. Global perturbation of
244 organic carbon cycling by river damming. *Nat. Commun.* 8, 15347.
245 doi:10.1038/ncomms15347
- 246 Mackereth, F.J.H., 1969. Short core sampler for subaqueous deposits. *Limnol. Oceanogr.* 14,
247 145–151.
- 248 Marín-Spiotta, E., Gruley, K.E., Crawford, J., Atkinson, E.E., Miesel, J.R., Greene, S.,
249 Cardona-Correa, C., Spencer, R.G.M., 2014. Paradigm shifts in soil organic matter
250 research affect interpretations of aquatic carbon cycling: Transcending disciplinary and
251 ecosystem boundaries. *Biogeochemistry* 117, 279–297. doi:10.1007/s10533-013-9949-7
- 252 Meyers, P.A., Lallier-Vergès, E., 1999. Lacustrine sedimentary organic matter of Late
253 Quaternary paleoclimates. *J. Paleolimnol.* 21, 345–372. doi:10.1023/A:1008073732192
- 254 Meyers, P. a, 2003. Application of organic geochemistry to paleolimnological reconstruction:
255 a summary of examples from the Laurention Great Lakes. *Org. Geochem.* 34, 261–289.
- 256 Mouchet, M.A., Paracchini, M.L., Schulp, C.J.E., Sturck, J., Verkerk, P.J., Verburg, P.H.,
257 Lavorel, S., 2016. Bundles of ecosystem (dis) services and multifunctionality across
258 European landscapes. *Ecol. Indic.* 73, 23–28. doi:10.1016/j.ecolind.2016.09.026. 73
- 259 Nakayama, T., 2017. Development of an advanced eco-hydrologic and biogeochemical
260 coupling model aimed at clarifying the missing role of inland water in the global
261 biogeochemical cycle. *J. Geophys. Res. Biogeosciences.*
- 262 Norris, C.E., Dungait, J.A.J., Joynes, A., Quideau, S.A., 2013. Biomarkers of novel
263 ecosystem development in boreal forest soils. *Org. Geochem.* 64, 9–18.

- 264 Owens, P.N., Blake, W.H., Gaspar, L., Gateuille, D., Koiter, A.J., Lobb, D.A., Petticrew,
265 E.L., Reiffarth, D.G., Smith, H.G., Woodward, J.C., 2016. Earth-Science Reviews
266 Fingerprinting and tracing the sources of soils and sediments : Earth and ocean science ,
267 geoarchaeological , forensic , and human health applications. *Earth Sci. Rev.* 162, 1–23.
268 doi:10.1016/j.earscirev.2016.08.012
- 269 Palazón, L., Latorre, B., Gaspar, L., Blake, W.H., Smith, H.G., Navas, A., 2015. Comparing
270 catchment sediment fingerprinting procedures using an auto-evaluation approach with
271 virtual sample mixtures. *Sci. Total Environ.* 532, 456–466.
272 doi:10.1016/j.scitotenv.2015.05.003
- 273 Panagos, P., Borrelli, P., Poesen, J., Ballabio, C., Lugato, E., Meusburger, K., Montanarella,
274 L., Alewell, C., 2015. The new assessment of soil loss by water erosion in Europe.
275 *Environ. Sci. Policy* 54, 438–447. doi:10.1016/j.envsci.2015.08.012
- 276 Parnell, A., Jackson, A., 2008. Stable Isotope Analysis in R [WWW Document]. URL
277 <https://cran.r-project.org/package=siar>
- 278 Puttock, A., Dungait, J.A.J., Macleod, C.J.A., Bol, R., Brazier, R.E., 2014. Woody plant
279 encroachment into grasslands leads to accelerated erosion of previously stable organic
280 carbon from dryland soils. *J. Geophys. Res. Biogeosciences* 119, 2345–2357.
281 doi:10.1002/2014JG002635.Received
- 282 Ranjan, R.K., Routh, J., Val Klump, J., Ramanathan, A.L., 2015. Sediment biomarker
283 profiles trace organic matter input in the Pichavaram mangrove complex, southeastern
284 India. *Mar. Chem.* 171, 44–57. doi:10.1016/j.marchem.2015.02.001
- 285 Raymond, P. a, Hartmann, J., Lauerwald, R., Sobek, S., McDonald, C., Hoover, M., Butman,
286 D., Striegl, R., Mayorga, E., Humborg, C., Kortelainen, P., Dürr, H., Meybeck, M.,
287 Ciais, P., Guth, P., 2013. Global carbon dioxide emissions from inland waters. *Nature*
288 503, 355–9. doi:10.1038/nature12760
- 289 Regnier, P., Friedlingstein, P., Ciais, P., Mackenzie, F.T., Gruber, N., Janssens, I. a., Laruelle,
290 G.G., Lauerwald, R., Luysaert, S., Andersson, A.J., Arndt, S., Arnosti, C., Borges, A.
291 V., Dale, A.W., Gallego-Sala, A., Godd eris, Y., Goossens, N., Hartmann, J., Heinze, C.,
292 Ilyina, T., Joos, F., LaRowe, D.E., Leifeld, J., Meysman, F.J.R., Munhoven, G.,
293 Raymond, P. a., Spahni, R., Suntharalingam, P., Thullner, M., 2013. Anthropogenic
294 perturbation of the carbon fluxes from land to ocean. *Nat. Geosci.* 6, 597–607.
295 doi:10.1038/ngeo1830
- 296 Reiffarth, D.G., Petticrew, E.L., Owens, P.N., Lobb, D.A., 2016. Sources of variability in
297 fatty acid (FA) biomarkers in the application of compound-specific stable isotopes
298 (CSSIs) to soil and sediment fingerprinting and tracing: A review. *Sci. Total Environ.*
299 565, 8–27. doi:10.1016/j.scitotenv.2016.04.137
- 300 Rickson, R.J., 2014. Can control of soil erosion mitigate water pollution by sediments? *Sci.*
301 *Total Environ.* 468–469, 1187–1197. doi:10.1016/j.scitotenv.2013.05.057
- 302 Schmidt, M.W.I., Torn, M.S., Abiven, S., Dittmar, T., Guggenberger, G., Janssens, I. a.,
303 Kleber, M., K ogel-Knabner, I., Lehmann, J., Manning, D. a. C., Nannipieri, P., Rasse,
304 D.P., Weiner, S., Trumbore, S.E., 2011. Persistence of soil organic matter as an
305 ecosystem property. *Nature* 478, 49–56. doi:10.1038/nature10386

- 306 Schoumans, O.F., Chardon, W.J., Bechmann, M.E., Gascuel-Oudou, C., Hofman, G.,
307 Kronvang, B., Rubæk, G.H., Ulén, B., Dorioz, J.M., 2014. Mitigation options to reduce
308 phosphorus losses from the agricultural sector and improve surface water quality: A
309 review. *Sci. Total Environ.* 468–469, 1255–1266. doi:10.1016/j.scitotenv.2013.08.061
- 310 Schroter, D., Cramer, W., Leemans, R., Arnell, N.W., Prentice, I.C., Arau, M.B., Bondeau,
311 A., Bugmann, H., Carter, T.R., Gracia, C.A., Vega-leinert, A.C. De, Erhard, M., Ewert,
312 F., Glendining, M., House, J.I., Klein, R.J.T., Lavorel, S., Kankaanpa, S., Lindner, M.,
313 Metzger, M.J., Meyer, J., Mitchell, T.D., Reginster, I., Rounsevell, M., 2005. Ecosystem
314 Service Supply and Vulnerability to Global Change in Europe.
- 315 Senbayram, M., Dixon, L., Goulding, K.W.T., B.R., 2008. Long-term influence of manure
316 and mineral nitrogen applications on plant and soil 15N and 13C values from the
317 Broadbalk Wheat Experiment. *Rapid Commun. Mass Spectrom.* 22, 1735–1740.
318 doi:10.1002/rcm.3548
- 319 Sherriff, S.C., Franks, S.W., Rowan, J.S., Fenton, O., Daire, Ó., 2015. Uncertainty-based
320 assessment of tracer selection , tracer non-conservativeness and multiple solutions in
321 sediment fingerprinting using synthetic and field data 2101–2116. doi:10.1007/s11368-
322 015-1123-5
- 323 Silliman, J.E., Schelske, C.L., 2003. Saturated hydrocarbons in the sediments of Lake
324 Apopka, Florida. *Org. Geochem.* 34, 253–260. doi:10.1016/S0146-6380(02)00169-9
- 325 Smith, H.G., Evrard, O., Blake, W.H., Owens, P.N., Smith, H.G., 2015. Preface —
326 Addressing challenges to advance sediment fingerprinting research 2033–2037.
327 doi:10.1007/s11368-015-1231-2
- 328 Tao, S., Eglinton, T.I., Montluçon, D.B., McIntyre, C., Zhao, M., 2016. Diverse origins and
329 pre-depositional histories of organic matter in contemporary Chinese marginal sea
330 sediments. *Geochim. Cosmochim. Acta* 191, 70–88. doi:10.1016/j.gca.2016.07.019
- 331 Team, R.C., 2014. R: A language and environment for statistical computing. R Foundation
332 for Statistical Computing, Vienna, Austria.
- 333 Tian, H., 2015. *Journal of Geophysical Research: Biogeosciences.* *J. Geophys. Res.*
334 *Biogeosciences* 120, 752–772. doi:10.1002/2014JG002760.Received
- 335 Tilman, D., Cassman, K.G., Matson, P.A., Naylor, R., Polasky, S., 2002. Agricultural
336 sustainability and intensive production practices. *Nature* 418, 671–677.
337 doi:10.1038/nature01014
- 338 Tolosa, I., Fiorini, S., Gasser, B., Martín, J., Miquel, J.C., 2013. Carbon sources in suspended
339 particles and surface sediments from the Beaufort Sea revealed by molecular lipid
340 biomarkers and compound-specific isotope analysis. *Biogeosciences* 10, 2061–2087.
341 doi:10.5194/bg-10-2061-2013
- 342 Torres, T., Ortiz, J.E., Martin-Sanchez, D., Arribas, I., Moreno, L., Ballesteros, B., Blazquez,
343 A., Dominguez, J.A., Estrealla, T.R., 2014. The long Pleistocene record from the Pero-
344 Oliva marshland (Alicante-Valencia, Spain), in: Martini, I.P., Wanless, H.R. (Ed.),
345 *Sedimentary Coastal Zones from High to Low Latitudes: Similarities and Differences.*
346 Geological Society of London, pp. 429–448.

- 347 Tranvik, L.J., Downing, J.A., Cotner, J.B., Loiselle, S.A., Striegl, R.G., Ballatore, T.J.,
348 Dillon, P., Finlay, K., Fortino, K., Knoll, L.B., Kortelainen, P.L., Kutser, T., Larsen, S.,
349 Laurion, I., Leech, D.M., McCallister, S.L., McKnight, D.M., Melack, J.M., Overholt,
350 E., Porter, J.A., Prairie, Y., Renwick, W.H., Roland, F., Sherman, B.S., Schindler, D.W.,
351 Sobek, S., Tremblay, A., Vanni, M.J., Verschoor, A.M., von Wachenfeldt, E.,
352 Weyhenmeyer, G.A., 2009. Lakes and reservoirs as regulators of carbon cycling and
353 climate. *Limnol. Oceanogr.* 54, 2298–2314. doi:10.4319/lo.2009.54.6_part_2.2298
- 354 Turnage, K.M., Lee, S.Y., Foss, J.E., Kim, K.H., Larsen, I.J., 1997. Comparison of soil
355 erosion and deposition rates using radiocesium, RUSLE, and buried soils in dolines in
356 East Tennessee. *Environ. Geol.* 29, 1–10.
- 357 Verheijen, F.G.A., Jones, R.J.A., Rickson, R.J., Smith, C.J., 2009. Tolerable versus actual
358 soil erosion rates in Europe. *Earth-Science Rev.* 94, 23–38.
359 doi:10.1016/j.earscirev.2009.02.003
- 360 Walling, D.E., 2013. The evolution of sediment source fingerprinting investigations in fluvial
361 systems. *J. Soils Sediments* 13, 1658–1675. doi:10.1007/s11368-013-0767-2
- 362 Wohl, E., Hall, R.O., Lininger, K.B., Sutfin, N.A., Walters, D.M., 2017. Carbon dynamics of
363 river corridors and the effects of human alterations. *Ecol. Monogr.* 87, 379–409.
364 doi:10.1002/ecm.1261
- 365 Zech, M., Krause, T., Meszner, S., Faust, D., 2013. Incorrect when uncorrected:
366 Reconstructing vegetation history using n-alkane biomarkers in loess-paleosol sequences
367 - A case study from the Saxonian loess region, Germany. *Quat. Int.* 296, 108–116.
368 doi:10.1016/j.quaint.2012.01.023
- 369 Zech, M., Rass, S., Buggle, B., Löffler, M., Zöller, L., 2012. Reconstruction of the late
370 Quaternary paleoenvironments of the Nussloch loess paleosol sequence, Germany, using
371 n-alkane biomarkers. *Quat. Res. (United States)* 78, 226–235.
372 doi:10.1016/j.yqres.2012.05.006
- 373 Zech, M., Zech, R., Morrill, H., Moretti, L., Glaser, B., Zech, W., 2009. Late Quaternary
374 environmental changes in Misiones, subtropical NE Argentina, deduced from multi-
375 proxy geochemical analyses in a palaeosol-sediment sequence. *Quat. Int.* 196, 121–136.
376 doi:10.1016/j.quaint.2008.06.006
- 377 Zhang, X.C. (John), Liu, B.L., 2016. Using multiple composite fingerprints to quantify fine
378 sediment source contributions: A new direction. *Geoderma* 268, 108–118.
379 doi:10.1016/j.geoderma.2016.01.031

380

Appendix 1 n-alkane data

Landuse	Source	Code*	n-alkane concentration $\mu\text{g g}^{-1}$ soil																		
			C1 5	C1 6	C1 7	C1 8	C1 9	C2 0	C2 1	C2 2	C2 3	C2 4	C2 5	C2 6	C27 8	C2 8	C29 0	C3 0	C31 2	C3 3	
grass	soil	1.1	0.36	0.50	0.32	0.61	n/a	0.28	0.38	0.46	0.32	0.26	0.66	0.16	1.49	0.33	3.79	0.59	6.30	0.32	3.82
grass	soil	1.2	0.36	0.87	0.55	0.77	n/a	0.43	0.71	0.38	0.38	0.18	0.82	0.36	1.61	0.50	3.93	0.57	6.63	0.35	3.85
grass	soil	1.3	0.57	0.50	0.37	0.59	n/a	0.69	0.58	0.19	0.06	0.05	0.62	0.08	1.17	0.24	4.31	0.51	7.32	0.18	4.19
grass	soil	1.4	0.18	0.27	0.23	0.37	n/a	0.40	0.35	0.19	0.27	0.28	0.38	0.03	0.73	0.48	2.20	0.34	4.13	0.25	2.15
grass	soil	1.5	0.07	0.19	0.16	0.50	n/a	0.34	0.34	0.23	0.53	0.17	0.75	0.37	1.53	0.55	2.98	0.61	5.29	0.45	3.37
arable	soil	2.1	0.28	0.33	0.29	0.56	n/a	0.82	0.40	0.15	0.09	0.39	0.37	0.09	1.28	0.27	2.37	0.35	3.81	0.24	1.98
arable	soil	2.2	0.09	0.08	0.09	0.27	n/a	0.19	0.21	0.17	0.28	0.19	0.39	0.14	0.84	0.24	2.13	0.34	3.65	0.23	1.99
arable	soil	2.3	0.11	0.28	0.24	0.43	n/a	0.42	0.26	0.12	0.30	0.18	0.38	0.19	0.90	0.25	2.00	0.38	3.71	0.23	2.00

arable	soil	2.4	0.08	0.10	0.12	0.26	n/a	0.31	0.17	0.10	0.30	0.18	0.43	0.18	1.08	0.28	1.93	0.27	3.34	0.24	1.81
arable	soil	3.3	0.08	0.09	0.11	0.24	n/a	0.21	0.26	0.10	0.27	0.20	0.61	0.19	1.57	0.37	3.02	0.40	4.33	0.26	2.30
woodland	soil	3.4	0.31	0.58	0.58	0.99	n/a	2.42	2.17	0.17	1.76	1.20	4.28	0.65	20.68	1.89	20.42	1.38	11.48	0.69	7.87
ley	soil	5.2	0.40	0.49	0.59	0.96	n/a	2.34	1.91	0.47	0.38	1.04	2.20	0.20	0.49	3.22	3.81	0.70	6.21	0.44	1.49
ley	soil	5.3	0.85	0.98	0.99	1.52	n/a	3.28	3.08	0.29	2.29	0.49	1.79	1.27	1.82	1.39	3.37	0.46	5.50	0.35	2.60
ley	soil	5.4	0.25	0.23	0.29	0.48	n/a	2.03	0.99	0.28	0.14	0.37	0.17	0.36	1.98	3.27	4.01	0.80	5.68	0.46	2.99
ley	soil	5.5	0.05	0.12	0.14	0.25	n/a	0.21	0.46	0.12	0.52	0.30	1.48	0.78	2.59	1.33	5.04	1.13	6.98	0.58	3.75
ley	soil	6.4	0.08	0.12	0.15	0.29	n/a	0.20	0.24	0.09	0.21	0.25	0.57	0.26	1.48	0.45	3.08	0.58	5.14	0.40	2.84
ley	soil	6.5	0.09	0.21	0.20	0.37	n/a	0.20	0.22	0.05	0.19	0.08	0.49	0.26	1.20	0.47	2.67	0.56	4.13	0.29	2.32
woodland	soil	6.6	0.06	0.11	0.14	0.35	n/a	0.28	0.44	0.64	1.19	0.96	3.48	1.48	14.55	2.01	15.31	1.09	7.12	0.65	3.48
grass	soil	8.5	0.10	0.10	0.10	0.20	n/a	0.10	0.10	0.10	0.10	0.20	0.60	0.30	1.71	0.80	3.14	0.70	4.78	0.30	2.10

			5	4	3	1		6	9	1	9	8	4	7		5		7		6	4
arable	soil	9.1	0.0 7	0.1 7	0.1 3	0.2 9	n/a	0.2 8	0.1 2	0.0 6	0.1 8	0.0 9	0.5 2	0.1 3	1.05	0.3 7	3.15	0.4 5	5.66	0.3 3	3.0 3
woodland	soil	9.7	0.0 4	0.0 4	0.0 5	0.0 9	n/a	0.1 3	0.2 8	0.1 6	0.4 8	0.3 0	2.0 7	0.6 0	10.7 0	1.3 4	9.02	0.6 0	4.97	0.3 3	4.5 7
arable	soil	10.5	0.0 7	0.1 2	0.1 4	0.3 5	n/a	0.2 4	0.2 5	0.1 7	0.1 1	0.1 0	0.3 2	0.0 7	0.77	0.1 8	1.71	0.2 6	2.83	0.1 8	1.4 1
ley	soil	11.5	0.2 7	0.2 6	0.1 8	0.3 4	n/a	0.4 9	0.4 1	0.1 3	0.1 4	0.1 3	0.0 8	0.1 4	0.44	0.1 3	1.54	0.1 8	2.72	0.1 4	1.0 8
ley	soil	11.6	0.0 7	0.0 8	0.1 1	0.2 5	n/a	0.2 2	0.2 4	0.1 9	0.1 1	0.0 5	0.5 7	0.0 6	0.69	0.2 1	2.10	0.2 5	3.57	0.1 8	1.6 7
ley	soil	11.7	0.2 1	0.1 2	0.1 9	0.3 1	n/a	0.8 4	0.7 2	0.0 5	0.1 9	0.3 3	0.1 4	0.1 8	0.88	0.2 3	2.23	0.5 1	3.21	0.2 2	1.2 2
grass	soil	11.8	0.1 1	0.0 3	0.0 5	0.1 8	n/a	0.1 9	0.4 5	0.1 8	0.6 6	0.5 6	1.4 3	0.6 6	4.75	0.9 0	6.35	0.6 8	4.21	0.3 0	1.6 5
woodland	soil	12.5	0.0 4	0.0 8	0.1 1	0.1 8	n/a	2.1 9	0.8 6	0.0 6	0.2 5	0.3 1	2.0 9	0.9 4	5.79	0.1 3	10.8 1	1.0 8	6.01	0.4 7	1.6 7
arable	soil	13.3	0.1 8	0.2 3	0.3 0	0.5 6	n/a	1.2 7	1.3 7	0.1 5	0.2 9	0.1 0	0.2 5	0.4 6	0.32	0.6 8	3.02	0.4 8	4.75	0.2 8	2.5 0
arable	soil	13.4	0.3 9	0.5 6	0.4 5	0.9 2	n/a	2.2 3	2.4 6	0.5 4	0.4 3	0.9 5	0.5 0	0.0 9	1.01	1.4 2	6.18	0.1 6	4.46	0.2 4	1.7 6

arable	soil	13.5	0.2 4	0.3 1	0.3 8	0.6 7	n/a	1.2 0	1.2 1	0.1 5	0.1 4	0.1 2	0.4 6	0.0 8	0.84	0.6 1	2.25	0.3 3	3.51	0.2 1	1.6 8
arable	soil	13.6	0.1 5	0.1 0	0.1 6	0.3 7	0.1 4	0.2 6	0.4 5	0.2 3	0.0 7	0.1 5	0.1 7	0.1 1	0.54	0.0 9	1.74	0.1 6	2.39	0.1 8	1.4 0
river	upstream	4	0.1 6	0.0 4	0.0 5	0.1 3	0.0 5	0.1 6	0.0 8	0.1 8	0.1 7	0.1 4	0.5 9	0.1 7	2.25	0.2 1	2.20	0.1 9	0.90	0.0 6	0.3 1
river	midstream	6	0.1 2	0.0 9	0.0 9	0.3 2	0.2 6	0.3 3	1.1 4	0.3 2	0.2 7	0.2 7	1.2 5	0.3 5	5.61	0.4 7	5.50	0.1 2	2.13	0.1 7	0.8 2
river	downstream	7	0.0 9	0.0 7	0.1 0	0.2 3	0.1 9	0.2 5	0.3 1	0.1 4	0.5 5	0.2 8	1.9 9	0.3 4	8.09	0.7 4	7.48	0.5 3	3.10	0.1 4	1.1 7
river	upstream	9	0.2 5	0.1 2	0.5 2	0.6 5	0.2 6	0.2 6	0.8 9	0.2 0	0.2 9	0.3 0	1.2 2	0.3 1	5.15	0.4 9	6.13	0.5 6	2.95	0.2 4	1.0 1
river	midstream	11	0.2 0	0.0 7	0.1 1	0.2 4	0.2 3	0.2 8	0.3 6	0.1 2	0.7 3	0.2 6	2.0 1	0.7 0	8.57	1.0 7	9.43	0.6 5	4.32	0.1 2	1.7 8
river	downstream	13	0.6 9	0.2 4	0.5 2	0.7 1	0.1 9	0.1 8	0.1 5	0.1 7	0.2 1	0.3 7	1.0 5	0.0 6	5.18	0.2 0	5.95	0.4 4	2.53	0.2 6	0.8 9
river	outlet	OUT	0.1 5	0.0 9	0.2 7	0.5 0	0.3 3	0.3 3	0.2 9	0.3 5	0.3 6	0.7 1	1.3 3	0.2 0	5.07	0.1 0	4.75	0.3 5	2.63	0.2 1	1.7 5
lake	1	0-4 cm	0.1 0	0.4 9	0.7 2	0.7 0	0.5 9	0.2 6	0.6 4	0.3 3	1.5 4	0.6 1	3.8 8	0.8 5	18.9 4	1.1 8	17.3 4	1.1 5	9.14	0.4 5	6.7 5
lake	2	4-8 cm	0.5	0.4	1.1	0.9	0.3	0.5	0.5	0.6	0.9	1.1	5.2	1.3	20.4	1.0	20.3	2.6	12.3	0.3	4.7

			4	5	7	3	4	6	4	5	7	8	4	9	8	6	0	6	9	1	5
lake	3	8-12 cm	0.1 6	0.5 0	1.0 4	0.8 7	0.9 8	0.3 3	1.0 5	0.4 2	1.4 3	0.5 7	4.9 6	0.7 5	19.0 2	0.3 1	18.5 9	1.2 9	11.5 2	0.2 7	6.1 8
lake	4	12-16 cm	0.3 1	0.3 3	0.4 3	0.7 0	0.5 4	0.0 8	0.6 2	1.0 3	1.2 0	2.8 6	5.1 5	0.8 9	21.9 7	0.1 3	20.7 4	0.5 0	14.3 9	0.1 6	5.7 0
lake	5	16-20 cm	0.1 3	0.4 4	0.6 6	0.6 0	1.0 9	1.5 1	1.1 4	0.3 6	2.2 3	0.4 6	4.7 6	0.6 4	17.2 7	2.1 5	17.8 2	1.5 9	12.4 0	1.0 3	4.1 2
lake	6	20-24 cm	0.4 2	0.4 8	0.7 0	0.6 2	0.7 2	3.1 6	1.9 7	0.3 9	2.7 3	2.9 1	0.5 7	0.8 0	15.7 2	0.8 0	16.1 1	0.4 4	12.8 5	0.0 5	6.5 8
lake	7	24-28 cm	0.1 1	0.3 1	0.7 0	1.0 6	1.6 2	3.3 5	1.5 0	0.2 2	3.5 2	0.4 0	4.6 0	1.1 6	16.6 8	3.9 7	15.7 8	0.4 5	12.3 2	1.3 8	4.4 7
lake	8	28-32 cm	0.4 1	0.5 9	1.2 7	1.0 5	1.1 6	2.0 7	0.8 1	1.0 0	2.0 3	3.9 4	4.5 0	0.1 7	17.2 1	2.2 6	15.3 6	0.4 5	12.0 9	0.9 9	3.5 5
lake	9	32-36 cm	0.5 6	0.8 2	1.9 6	1.5 8	1.2 1	1.8 5	0.8 9	1.2 6	1.9 8	3.8 7	5.6 2	0.6 3	18.9 9	0.5 9	17.7 7	0.8 9	12.8 2	0.7 9	4.0 3
lake	10	36-40 cm	0.1 9	0.3 8	3.5 4	0.7 5	1.6 8	0.1 6	1.0 4	0.4 0	1.5 8	1.2 1	4.6 9	1.0 5	13.6 0	3.2 5	15.7 3	1.3 6	13.1 0	0.7 7	5.8 0
lake	11	40-44 cm	0.0 3	0.1 2	1.4 9	0.3 1	0.6 2	0.5 0	0.5 3	0.2 0	1.4 7	1.3 5	2.4 5	0.5 6	7.07	1.5 2	9.95	0.9 3	9.05	0.4 3	2.9 7
lake	12	44-48 cm	0.2 0	0.2 7	1.6 7	1.1 0	1.0 0	1.6 6	0.7 8	0.5 6	2.0 8	1.3 8	3.6 2	0.7 8	10.4 2	3.2 3	13.8 8	1.0 6	12.8 8	0.5 4	4.3 3

* transect and core number for soil
samples

location for stream bed sediment
samples

depth increment for lake
core

Appendix 2 – stable isotope data

Landuse	Source	Code	% N	$\delta^{15}\text{N}$ ‰	% C	$\delta^{13}\text{C}$ ‰
grass	soil	1.1	0.42	5.20	4.12	-27.81
grass	soil	1.2	0.49	5.78	5.53	-27.27
grass	soil	1.3	0.57	3.26	6.50	-28.33
grass	soil	1.4	0.44	6.37	4.13	-27.34
grass	soil	1.5	0.61	6.66	6.02	-28.02
arable	soil	2.1	0.40	4.81	4.14	-27.01
arable	soil	2.2	0.30	3.72	2.99	-28.00
arable	soil	2.3	0.38	7.59	3.99	-27.00
arable	soil	2.4	0.37	5.05	3.55	-26.98
arable	soil	3.1	0.39	4.97	3.56	-27.85
arable	soil	3.2	0.37	5.93	3.66	-27.05
arable	soil	3.3	0.25	4.80	2.57	-27.69
woodland	soil	3.4	0.84	5.56	10.36	-28.11
woodland	soil	3.4b	0.69	5.63	8.76	-27.71
woodland	soil	3.4c	0.49	4.70	6.92	-28.35
ley	soil	4.1	0.36	5.07	3.35	-28.27
ley	soil	4.2	0.41	5.35	4.08	-28.13
ley	soil	4.3	0.47	5.25	4.78	-28.30
ley	soil	4.4	0.43	5.09	4.10	-28.43
ley	soil	5.1	0.41	5.10	4.17	-27.95
ley	soil	5.2	0.40	5.28	3.69	-28.37
ley	soil	5.3	0.41	5.69	4.09	-28.01
ley	soil	5.4	0.43	5.20	4.19	-28.52

ley	soil	5.5	0.57	4.90	5.87	-28.58
ley	soil	6.1	0.35	4.87	3.15	-27.99
ley	soil	6.2	0.32	3.82	3.00	-28.72
ley	soil	6.3	0.33	4.63	3.02	-28.14
ley	soil	6.4	0.40	4.85	3.75	-28.41
ley	soil	6.5	0.44	3.96	4.18	-28.52
woodland	soil	6.6	0.64	5.58	7.16	-28.65
arable	soil	7.1	0.35	5.53	3.25	-27.26
arable	soil	7.2	0.21	5.39	1.83	-27.29
ley	soil	7.3	0.23	5.69	2.20	-26.96
ley	soil	7.4	0.31	6.07	2.70	-27.47
ley	soil	7.5	0.38	5.71	3.52	-27.88
grass	soil	7.6	0.59	6.27	5.56	-28.28
grass	soil	7.7	0.48	7.07	5.10	-28.14
ley	soil	8.1	0.47	5.86	4.60	-28.28
ley	soil	8.2	0.38	6.79	3.42	-28.17
arable	soil	8.3	0.32	6.11	2.78	-27.29
arable	soil	8.4	0.32	5.53	2.92	-27.42
grass	soil	8.5	0.68	5.20	6.73	-28.38
grass	soil	8.6	0.71	4.16	6.88	-28.33
arable	soil	9.1	0.35	5.07	3.40	-27.78
arable	soil	9.2	0.32	5.90	2.90	-28.19
grass	soil	9.3	0.92	7.29	8.28	-29.15
grass	soil	9.4	0.60	4.99	5.77	-28.42
grass	soil	9.5	0.48	5.33	4.48	-28.38
grass	soil	9.6	0.47	6.24	4.45	-27.62

woodland	soil	9.7	0.50	5.94	4.98	-28.51
ley	soil	10.1	0.38	6.89	3.22	-28.42
arable	soil	10.2	0.31	6.38	2.64	-27.26
arable	soil	10.3	0.35	5.43	2.90	-27.56
arable	soil	10.4	0.27	5.39	2.34	-27.86
arable	soil	10.5	0.34	4.95	2.98	-27.82
woodland	soil	10.6	0.77	3.80	9.59	-28.25
arable	soil	11.1	0.22	3.62	2.08	-27.85
arable	soil	11.3	0.31	5.20	2.72	-28.00
arable	soil	11.4	0.35	5.17	2.89	-27.84
ley	soil	11.5	0.28	5.95	2.12	-27.69
ley	soil	11.6	0.37	6.01	3.45	-28.09
ley	soil	11.7	0.32	5.33	2.56	-27.79
grass	soil	11.8	0.43	4.10	4.80	-28.84
ley	soil	12.1	0.43	7.64	3.67	-28.82
ley	soil	12.3	0.41	6.66	3.56	-28.46
ley	soil	12.4	0.38	6.03	3.06	-28.23
woodland	soil	12.5	0.50	1.77	8.68	-28.02
arable	soil	13.1	0.31	6.09	2.64	-27.74
arable	soil	13.2	0.38	6.52	3.36	-27.87
arable	soil	13.3	0.30	6.24	2.56	-28.13
arable	soil	13.4	0.29	5.38	2.46	-27.65
arable	soil	13.5	0.29	4.39	2.25	-27.95
arable	soil	13.6	0.32	5.91	2.63	-27.69
arable	soil	14.1	0.29	5.57	2.24	-27.84
arable	soil	14.2	0.31	5.59	2.73	-27.74

arable	soil	14.3	0.34	5.71	2.95	-27.04
arable	soil	14.4	0.37	6.12	3.28	-27.18
arable	soil	14.5	0.38	6.40	3.47	-28.00
river	Upstream	4	0.11	3.41	1.16	-28.15
river	Midstream	6	0.16	3.34	2.08	-28.23
river	Downstream	7	0.21	4.98	2.74	-28.71
river	Upstream	9	0.24	6.48	2.82	-28.34
river	Midstream	11	0.28	4.63	3.68	-28.28
river	Downstream	13	0.19	4.45	2.32	-28.33
river	outlet	OUT	0.13	4.52	1.55	-27.91
lake	0-2 cm	1_1	0.76	6.58	8.32	-28.16
lake	0-2 cm	1_1	0.75	6.31	8.44	-28.20
lake	2-4 cm	1_1	0.76	6.68	8.46	-28.18
lake	4-6 cm	1_2	0.72	6.28	7.84	-28.27
lake	6-8 cm	1_3	0.66	5.76	7.71	-28.24
lake	8-10 cm	1_4	0.69	6.26	7.85	-27.99
lake	10-12 cm	1_5	0.67	6.36	7.53	-28.04
lake	12-14 cm	1_6	0.69	6.17	7.41	-27.99
lake	14-16 cm	1_7	0.68	6.90	7.37	-27.97
lake	16-18 cm	1_8	0.69	6.72	7.65	-27.96
lake	18-20 cm	1_9	0.78	6.94	9.40	-27.73
lake	22-24 cm	1_10	0.77	6.69	9.15	-27.21
lake	24-26 cm	1_11	0.80	6.78	8.50	-27.23
lake	26-28 cm	1_12	0.72	6.33	7.66	-27.33
lake	28-30 cm	1_13	0.78	6.25	8.41	-27.09
lake	32-34 cm	1_14	0.72	6.26	7.58	-27.16

lake	34-36 cm	1_15	0.74	6.63	7.75	-27.15
lake	36-38 cm	1_16	0.73	6.87	7.74	-27.19
lake	38-40 cm	1_17	0.65	6.05	7.06	-27.44
lake	40-42 cm	1_18	0.63	6.58	6.58	-27.68
lake	42-44 cm	1_19	0.57	5.94	5.95	-28.01
lake	44-46 cm	1_20	0.54	6.10	5.72	-27.83
lake	46-48 cm	1_21	0.61	5.88	6.39	-27.58
lake	48-50 cm	1_22	0.58	6.03	6.04	-27.35
lake	50-52 cm	1_23	0.56	6.06	5.51	-27.40
lake	52-54 cm	1_24	0.64	5.76	5.89	-26.86
lake	54-56 cm	1_25	0.62	5.73	5.80	-26.84